Table 2 Clinical features of the three cases

	Case 1	Case 2	Case 3
Age at onset (years)	61	59	42
Gender	Male	Female	Female
Disease duration (months)	25	39	228
Site of initial symptom	Distal part of the right lower limb	Left lower limb	Distal part of the left lower limb
Deep tendon reflex at onset			
Upper limb (right/left)	Normal/normal	Increased/increased	Normal/normal
Patellar (right/left)	Normal/normal	Increased/increased	Normal/decreased
Achilles (right/left)	Absent/absent	Absent/absent	Decreased/absent
Babinski's sign (right/left)	Negative/negative	Positive/positive	Negative/negative
Upper motor neuron sign (throughout the course)	Present	Present	Absent
Bulbar symptom (initially/eventually)	Absent/present	Absent/present	Absent/present
Clinical diagnosis	Pseudopolyneuritic form of ALS	Pseudopolyneuritic form of ALS	Spinal progressive muscular atrophy

Table 3 Neuropathological findings of the three cases

	Case 1	Case 2	Case 3
Brain weight (g)	1410 (after fixation)	1310 (before fixation)	1230 (before fixation)
Lower motor neuron loss			
Hypoglossal nucleus	Moderate	Moderate	Moderate
Spinal cord	Severe at all levels	Severe at all levels	Severe at all levels
Distribution of Bunina bodies	Trigeminal nucleus, hypoglossal nucleus, anterior horn (C6, C8, L3, S2)	Hypoglossal nucleus	–
Corticospinal tract degeneration			
Posterior limb of internal capsule	–	–	–
Midbrain	+	–	–
Medulla oblongata	+	+	–
Cervical cord	+	+	–
Thoracic cord	+	+	–
Lumbar cord	+	+	+

walk at age 62. Subsequently, he developed muscle weakness of the bilateral upper limbs and dysarthria, and was admitted to our hospital 1 year and 10 months after onset. Neurological examination demonstrated mild facial palsy. Tongue atrophy or fasciculation was not apparent. Muscle weakness was also demonstrated in all four limbs, and the distal part of the lower limbs showed complete paralysis. Muscle atrophy was prominent in the bilateral tibialis anterior muscles. ATR was absent, and the patellar tendon reflex was within normal limits on the right side, and was increased on the left side. The bilateral upper limbs showed hyper-reflexia. Muscle biopsy showed neurogenic changes. A clinical diagnosis of the pseudopolyneuritic form of ALS was made. The patient refused artificial respiratory support and died of respiratory failure.

Neuropathological findigs. Microscopically, the lateral part of the anterior horn was atrophic in the lumbar and cervical cord (Fig. 1a,d). Severe LMN loss was demonstrated throughout the whole spinal cord (Fig. 1a,c,d). A few neurons were demonstrated in the intermediate zone in the lumbar cord. Moderate neuronal loss was demonstrated in the hypoglossal nucleus (Fig. 1e) and trigeminal motor nucleus. Myelin pallor in the CST was demonstrated in the whole spinal cord (Fig. 1a,b), medulla oblongata and midbrain, but was not obvious in the internal capsule. In the anterior funiculus of the thoracic cord, myelin pallor was demonstrated beyond the CST[16] (Fig. 1b). Neuronal loss was not apparent in the cerebrum, although there was sparse accumulation of lipid-laden macrophages in the shape of a Betz cell in the precentral gyrus. Bunina bodies were demonstrated in the LMNs. Only one ubiquitin-positive skein-like neuronal cytoplasmic inclusion (NCI) was found in the anterior horn of the cervical cord. TDP-43-positive NCIs were demonstrated in the entorhinal, transentorhinal and occipitotemporal cortices, amygdala, globus pallidus, inferior olivary nucleus, reticular formation of the medulla, and anterior horn of the thoracic, lumbar and sacral cords. Glial cytoplasmic inclusions (GCIs) were distributed more frequently and extensively, that is, in the frontal, temporal, and parietal lobe, amygdala, globus pallidus, thalamus, cerebral peduncle, trigeminal motor nucleus, pontine nucleus, hypoglossal nucleus, inferior olivary nucleus, reticular formation of the medulla,

Table 4 Distribution and severity of TDP-43 pathology across scanned central nervous system regions

	Case 1		Case 2		Case 3	
	NCI	GCI	NCI	GCI	NCI	GCI
Cerebrum						
Cingulate gyrus cortex	0	0	0	0	0	0
Cingulate white matter		0		0		0
Frontal cortex	0	1	0	1	0	0
Frontal white matter		1		0		0
Motor cortex	0	2	0	1	0	0
Motor white matter		2		0		0
Anterior parietal cortex	0	1	0	0	0	0
Anterior parietal white matter		1		0		0
Amygdala	1	2	0	0	0	0
Dentate gyrus	0	0	0	0	0	0
CA/subiculum	0	0	0	0	0	0
Entorhinal cortex	1	1	0	0	0	0
Entorhinal white matter		1		0		0
Insular cortex	0	1	0	0	0	0
Insular white matter		0		0		0
Temporal cortex	1	1	0	0	0	0
Temporal white matter		1		0		0
Striatum	0	0	0	0	0	0
Globus pallidus	1	1	0	0	0	0
Thalamus	0	1	0	0	0	0
Posterior limb of internal capsule		0		0		0
Midbrain						
Reticular formation	0	0	NA		0	0
Red nucleus	0	0	0	0	0	0
Substantia nigra	0	0	0	0	0	0
Cerebral peduncle		1		0		0
Pons						
Trigeminal nucleus	0	2	1	0	NA	
Facial nucleus	NA		NA		1	0
Reticular formation	0	0	0	0	0	0
Pontine nucleus	0	1	0	1	0	0
Pramidal tract		0		0		0
Medulla oblongata						
Hypoglossal nucleus	0	1	1	1	1†	1
Inferior olivary nucleus	1	1	0	1	0‡	0
Reticular formation	1	2	1	2	0	0
Pyramid		1		1	0	0
Spinal cord						
Anterior horn	1	2	1	0	0	0
Ventral corticospinal tract		1		0		0
Lateral corticospinal tract		1		0		0

†Dystrophic neurites were also found. ‡TDP-43-positive round structures were found in the neuropil. In case 3, the distribution and severity were evaluated using anti-TDP-43C [405–414] antibody. 0, no pathology; 1, rare to mild pathology; 2, moderate to severe pathology; GCI, glial cytoplasmic inclusion; NA, tissue not available; NCI, neuronal cytoplasmic inclusion.

pyramid, and whole spinal cord. In the cerebrum, numerous GCIs were demonstrated in the precentral gyrus (Fig. 2). These were frequently seen in the deep layers of the cortex, and less distributed in the superficial layer and subcortical white matter. In the spinal cord, numerous GCIs were seen in the anterior horn of the lumbar cord (Fig. 1f).

Case 2

Clinical course. A 59-year-old Japanese woman developed weakness in the left leg. Ten months after onset, she was admitted to the Department of Neurology of a general hospital. Neurological examination showed atrophy and fasciculation of the left lower limb, especially in the distal part. ATR was absent bilaterally, whereas patellar and upper-limb tendon reflexes were increased bilaterally. A clinical diagnosis of the pseudopolyneuritic form of ALS was made. At age 62, she was emergently admitted to our hospital because of dyspnea. Neurological examination demonstrated atrophy and fasciculation of the tongue, dysarthria, dysphagia, and muscle atrophy and weakness in all four limbs. ATR was absent, and patellar and upper-limb tendon reflexes were decreased. There was neither character change nor dementia. The patient refused artificial respiratory support and died of respiratory failure approximately 18 days after admission.

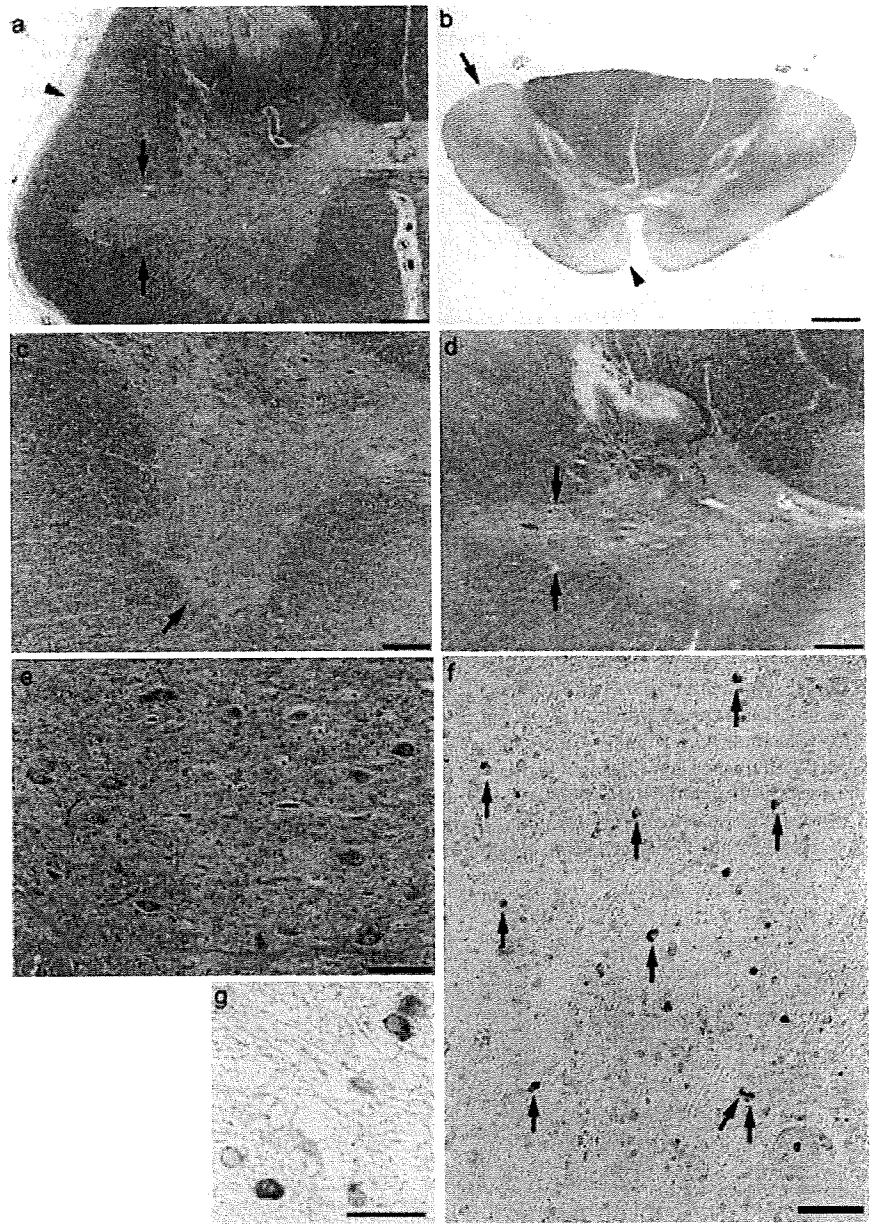

Fig. 1 Front and back diameter of the lateral part of the anterior horn was reduced in lumbar segment 5 (a, arrows). Motor neurons had almost disappeared (a). Lateral corticospinal tract (CST) showed myelin pallor and atrophy (a, arrowhead). In thoracic segment 10, myelin pallor was seen in the lateral (b, arrow) and anterior (b, arrowhead) CST with extension outside the CST in the anterior funiculus. High-power view demonstrated that motor neurons had almost disappeared (c, arrow). Front and back diameter of the lateral part of the anterior horn was reduced in cervical segment 6 (d, arrows). Motor neurons had almost disappeared (d). Moderate neuronal loss was seen in the hypoglossal nucleus (e). Glial cytoplasmic inclusions (GCIs) were frequently seen in the anterior horn of lumbar segment 5, whereas there were no neuronal cytoplasmic inclusions (NCIs) in this region (f). High-power view (g). a–e KB stain: f, g phospholylated TDP-43 (pS409/410). Scale bar a 500 μm, b 1 mm, c 200 μm, d 500 μm, e 100 μm, f 50 μm, g 20 μm.

Neuropathological findigs. Microscopically, the lateral part of the anterior horn of the lumbar cord was atrophic. Severe LMN loss was demonstrated throughout the whole spinal cord. In the anterior horn of the lumbar cord, a few neurons were demonstrated in the medial motor nucleus and intermediate zone, whereas the lateral motor nucleus showed complete neuronal loss. Moderate neuronal loss was demonstrated in the hypoglossal nucleus and trigeminal motor nucleus. Myelin pallor in the CST was demonstrated in the whole spinal cord and medulla oblongata, but was not obvious in the midbrain and internal capsule. Bunina bodies were seen in the hypoglossal nucleus. There was sparse accumulation of lipid-laden macrophages in the shape of a Betz cell in the precentral gyrus. Neuronal loss was evident in the basolateral area of the amygdala, and substantia nigra. Ubiquitin-immunoreactive NCIs were demonstrated in the hippocampal dentate granular cells, hypoglossal nucleus, and anterior horn of the lumbar cord. They were not demonstrated in the amygdala or substantia nigra. TDP-43-positive NCIs were sparsely demonstrated in the trigeminal motor nucleus, hypoglossal nucleus, reticular formation of the medulla, and anterior horn of the lumbar cord. Unexpectedly, ubiquitin-immunoreactive NCIs in the hippocampal dentate granular cells were negative for all kinds of anti-TDP-43 antibodies. These were also negative for FUS, AT8, and α-synuclein. TDP-43-positive GCIs were frequently seen in the reticular formation of the medulla, and were sparse in the cortex of the

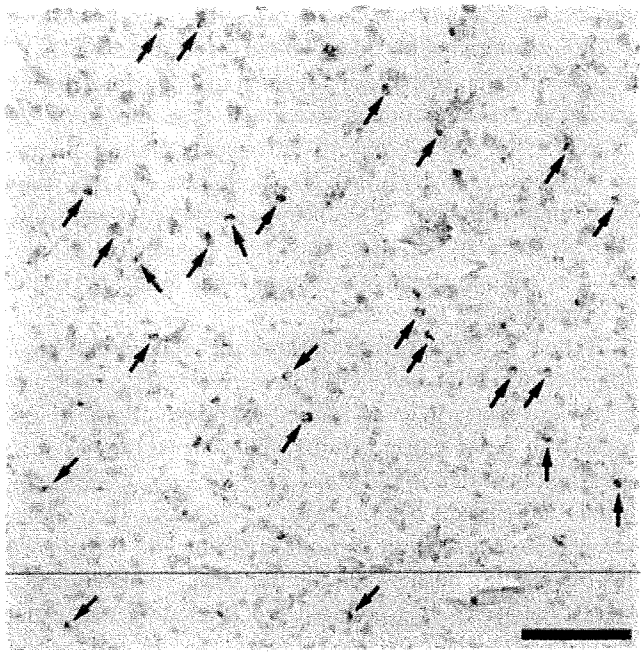

Fig. 2 A red line shows the boundary between the gray and white matter of the precentral gyrus. Immunohistochemistry using anti-phosphorylated TDP-43 (pS409/410) antibodies demonstrated that glial cytoplasmic inclusions (GCIs) (arrows) were frequently seen in the deep layer of the cortex, and less distributed in the subcortical white matter. Neuronal cytoplasmic inclusions (NCIs) were not apparent. Scale bar 50 μm.

precentral gyrus, pontine nucleus, hypoglossal nucleus, inferior olivary nucleus and pyramid, and were not demonstrated in the spinal cord.

Case 3

Clinical course. A 42-year-old Japanese woman developed muscle weakness in the distal part of the left lower limb. Neurological examination at age 46 demonstrated muscle atrophy and weakness in the left lower limb with distal predominance. The left ATR was absent, and the right ATR and left patellar tendon reflex were decreased. A diagnosis of lumbar disc herniation was made, and laminectomy of the lumbar segment 4–5 was performed. However, there was no improvement, and she began to use a cane while walking. At age 49, she developed muscle weakness of the right lower limb and the distal part of the bilateral upper limbs. She died of suffocation probably related to bulbar palsy at age 61. There were no UMN signs throughout the clinical course.

Neuropathological findings. Microscopically, severe LMN loss was demonstrated throughout the whole spinal cord. Small neurons of the intermediate zone in the lumbar cord were also lost. Moderate neuronal loss was demonstrated in the hypoglossal nucleus and facial nucleus. Bunina bodies were not demonstrated. Myelin pallor and gliosis were seen in the CST of the lumbar cord (Fig. 3a), and loss

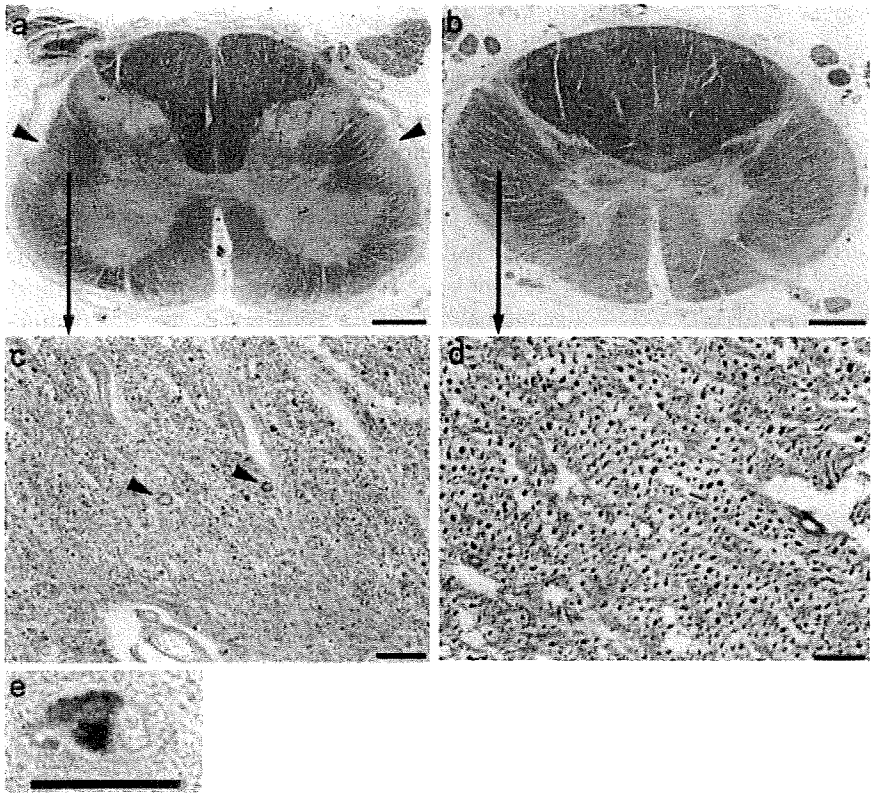

Fig. 3 Myelin pallor was demonstrated in the lateral corticospinal tract (CST) in lumbar segment 5 (a, arrowheads), but was not apparent in thoracic segment 10 (b). Axons were severely lost, and spheroids (c, arrowheads) were seen in the right lateral CST of lumbar segment 5 (c). In contrast, axons were preserved in the right lateral CST of the thoracic segment 10 (d). An neuronal cytoplasmic inclusion (NCI) was demonstrated in the hypoglossal nucleus (e). a, b KB stain; d, e neurofilament; e TDP-43C [405–414], Scale bar a, b 1 mm; c–e 50 μm.

of axons was also demonstrated by anti-neurofilament antibodies (Fig. 3c). They were not apparent in the CST of the thoracic and cervical cord (Fig. 3b,d), brainstem, and internal capsule. There was sparse accumulation of lipid-laden macrophages in the shape of a Betz cell in the pre-central gyrus. Immunohistochemical re-examination using anti-ubiquitin antibodies demonstrated a skein-like NCI in the hypoglossal nucleus, although it was not demonstrated previously.[14] Using two kinds of anti-phosphorylated TDP-43 antibodies, there were no TDP-43-positive structures, although anti-TDP-43C [405–414]) antibodies detected NCIs in the facial nucleus and hypoglossal nucleus (Fig. 3e). Dystrophic neurites and GCIs were also seen in the hypoglossal nucleus, and round structures were observed in the neuropil of the inferior olivary nucleus. NCIs in the facial nucleus and hypoglossal nucleus were also demonstrated by another phosphorylation-independent antibody. There were no TDP-43-positive structures in the cerebrum or spinal cord. There were no cystatin C immunoreactive Bunina bodies.

LMN loss of the spinal cord in the control cases

Severe LMN loss in the cervical cord was demonstrated in 13 of 15 cases, whereas that in the lumbar cord was seen only in two of four cases of lower-limb onset ALS, and in three of 11 cases of upper-limb onset ALS. In the cases showing severe LMN loss in the lumbar cord, small neurons in the intermediate zone of the anterior horn were also decreased in the lumbar cord.

DISCUSSION

The pseudopolyneuritic form of ALS is a subtype of ALS characterized by distal weakness of the unilateral lower limb and absence of ATR at disease onset.[4–6] Recognition of this form of ALS is important for clinicians because the combination of distal weakness of the lower limb and absence of ATR usually suggests peripheral neuropathy. In clinical practice, identification of the hyper-reflexia in the knees and/or upper limbs may be a key in making a diagnosis of ALS, although exceptional cases such as our case 3 may not show UMN signs.

Our three patients showed weakness of the unilateral lower limb with distal dominance and absence of ATR while other clinical features were variable among cases. At autopsy, severe LMN loss throughout the whole spinal cord seen in the three cases was concordant with the findings reported by Nishigaki *et al.*[11] However, this finding does not appear to be specific for this form because there were similar findings in five of 15 cases examined as controls. Probably, early and severe involvement of motor neurons in lumbar segment 5 and/or sacral segment 1 results in muscle weakness of the distal lower limb and absence of ATR, causing the pseudopolyneuritic form of ALS. In other words, this form does not seem to comprise a distinct pathological entity but is one phenotype based on the characteristic clinical features at onset. Among the cases showing severe LMN loss in the lumbar cord in this study, we could not find any differences between the pseudopolyneuritic form and control cases with regard to the small neurons in the intermediate zone of the anterior horn of the lumbar cord.

Reflecting the severe LMN loss throughout the whole spinal cord in our cases, TDP-43-positive NCIs in the spinal cord were sparse in cases 1 and 2, and were absent in case 3. On the other hand, various TDP-43 pathologies were also demonstrated in our three cases. In case 1, unlike the other two cases, TDP-43-positive inclusions were extensively demonstrated throughout the brain and spinal cord. In the anterior horn of the lumbar cord, numerous GCIs were demonstrated despite severe LMN loss, suggesting that glial cells were affected even after the LMNs were lost. In case 2, ubiquitinated protein in the hippocampal dentate granular cells was negative for TDP-43, FUS, AT8, and α-synuclein, therefore a yet unknown protein may have been involved in this region. In case 3, TDP-43-positive structures were demonstrated only in the brainstem, and such a limited distribution may be consistent with the findings of ALS showing prolonged disease duration.[17]

Finally, in case 3, we could not make a clinical diagnosis of ALS because there were no UMN signs throughout the clinical course. Involvement of the CST might have been detected if motor-evoked potentials had been examined.[6] At autopsy, CST degeneration was mild, and this finding appeared to correspond to the absence of UMN signs and prolonged disease duration.[17] There has been a long controversy as to whether sporadic spinal progressive muscular atrophy (SPMA) is a variant of ALS or a distinct disease. Usually, a clinical diagnosis of SPMA is made when the patient does not show UMN signs. However, at autopsy UMN pathology[17–20] and/or Bunina bodies[17] are demonstrated in some patients, suggesting that the underying pathology is similar to that of ALS in some patients with SPMA. In addition, we could not completely exclude the possibility that mutation in superoxide dismutase-1 (SOD1) was present in case 3. Although this possibility seemed unlikely based on the absence of a family history and presence of TDP-43-positive inclusions,[21,22] clinicians should know that some familial ALS cases with the SOD1 mutation show clinical features similar to those of case 3.[23–26]

ACKNOWLEDGEMENTS

The authors thank Ms Hiromi Kondo, Yoko Shimomura, and Chie Haga (Tokyo Institute of Psychiatry) for their

excellent technical assistance. This work was supported by a grant-in-aid for scientific research from the Ministry of Education, Culture, Sports, Science and Technology (14570957) and a research grant from the Zikei Institute of Psychiatry.

REFERENCES

1. Nalini A, Thennarasu K, Gourie-Devi M, Shenoy S, Kulshreshtha D. Clinical characteristics and survival pattern of 1,153 patients with amyotrophic lateral sclerosis: experience over 30 years from India. *J Neurol Sci* 2008; **272**: 60–70.
2. Ravits J, Laurie P, Fan Y, Moore DH. Implications of ALS focality: rostral-caudal distribution of lower motor neuron loss postmortem. *Neurology* 2007; **68**: 1576–1582.
3. Ince PG. Neuropathology. In: Brown RJ, Meininger V, Swash M, eds. *Amyotrophic Laeral Sclerosis*. London: Martin Dunitz, 2000; 83–112.
4. Patrikios JS. *Contribution À l'Étude Des Formes Cliniques Et De l'Anatomie Pathologique De La Sclérose Latérale Amyotrophique*. Paris University, 1918.
5. Bonduelle M. Amyotrophic lateral sclerosis. In: Vinken PJ, Bruyn GW, eds. *Handbook of Clinical Neurology*. 22. Amsterdam: North-Holland, 1975; 281–338.
6. Cappellari A, Ciammola A, Silani V. The pseudopolyneuritic form of amyotrophic lateral sclerosis (Patrikios' disease). *Electromyogr Clin Neurophysiol* 2008; **48**: 75–81.
7. Guidetti D, Bondavalli M, Sabadini R *et al.* Epidemiological survey of amyotrophic lateral sclerosis in the province of Reggio Emilia, Italy: influence of environmental exposure to lead. *Neuroepidemiology* 1996; **15**: 301–312.
8. Mortara P, Bardelli D, Leone M, Schiffer D. Prognosis and clinical varieties of ALS disease. *Ital J Neurol Sci* 1981; **2**: 237–242.
9. Salemi G, Fierro B, Arcara A, Cassata M, Castiglione MG, Savettieri G. Amyotrophic lateral sclerosis in Palermo, Italy: an epidemiological study. *Ital J Neurol Sci* 1989; **10**: 505–509.
10. Wijesekera LC, Mathers S, Talman P *et al.* Natural history and clinical features of the flail arm and flail leg ALS variants. *Neurology* 2009; **72**: 1087–1094.
11. Nishigaki S, Ando K, Nagata Y, Hirose K. Pseudopolyneuritic form of amyotrophic lateral sclerosis. *Rinsho Shinkeigaku* 1973; **13**: 377–384.
12. Terao S, Sobue G, Hashizume Y, Mitsuma T, Takahashi A. Disease-specific patterns of neuronal loss in the spinal ventral horn in amyotrophic lateral sclerosis, multiple system atrophy and X-linked recessive bulbospinal neuronopathy, with special reference to the loss of small neurons in the intermediate zone. *J Neurol* 1994; **241**: 196–203.
13. Tsuchiya K, Shintani S, Kikuchi M *et al.* Sporadic amyotrophic lateral sclerosis of long duration mimicking spinal progressive muscular atrophy: a clinicopathological study. *J Neurol Sci* 1999; **162**: 174–178.
14. Hasegawa M, Arai T, Nonaka T *et al.* Phosphorylated TDP-43 in frontotemporal lobar degeneration and amyotrophic lateral sclerosis. *Ann Neurol* 2008; **64**: 60–70.
15. Neumann M, Rademakers R, Roeber S, Baker M, Kretzschmar HA, Mackenzie IR. A new subtype of frontotemporal lobar degeneration with FUS pathology. *Brain* 2009; **132**: 2922–2931.
16. Hayashi S, Sakurai A, Amari M, Okamoto K. Pathological study of the diffuse myelin pallor in the anterolateral columns of the spinal cord in amyotrophic lateral sclerosis. *J Neurol Sci* 2001; **188**: 3–7.
17. Nishihira Y, Tan CF, Hoshi Y *et al.* Sporadic amyotrophic lateral sclerosis of long duration is associated with relatively mild TDP-43 pathology. *Acta Neuropathol* 2009; **117**: 45–53.
18. Brownell B, Oppenheimer DR, Hughes JT. The central nervous system in motor neurone disease. *J Neurol Neurosurg Psychiatry* 1970; **33**: 338–357.
19. Ince PG, Evans J, Knopp M *et al.* Corticospinal tract degeneration in the progressive muscular atrophy variant of ALS. *Neurology* 2003; **60**: 1252–1258.
20. Sasaki S, Iwata M. Immunocytochemical and ultrastructural study of the motor cortex in patients with lower motor neuron disease. *Neurosci Lett* 2000; **281**: 45–48.
21. Tan CF, Eguchi H, Tagawa A *et al.* TDP-43 immunoreactivity in neuronal inclusions in familial amyotrophic lateral sclerosis with or without SOD1 gene mutation. *Acta Neuropathol* 2007; **113**: 535–542.
22. Mackenzie IR, Bigio EH, Ince PG *et al.* Pathological TDP-43 distinguishes sporadic amyotrophic lateral sclerosis from amyotrophic lateral sclerosis with SOD1 mutations. *Ann Neurol* 2007; **61**: 427–434.
23. Aoki M, Ogasawara M, Matsubara Y *et al.* Familial amyotrophic lateral sclerosis (ALS) in Japan associated with H46R mutation in Cu/Zn superoxide dismutase gene: a possible new subtype of familial ALS. *J Neurol Sci* 1994; **126**: 77–83.
24. Ohi T, Saita K, Takechi S *et al.* Clinical features and neuropathological findings of familial amyotrophic lateral sclerosis with a His46Arg mutation in Cu/Zn superoxide dismutase. *J Neurol Sci* 2002; **197**: 73–78.

25. Ohi T, Nabeshima K, Kato S, Yazawa S, Takechi S. Familial amyotrophic lateral sclerosis with His46Arg mutation in Cu/Zn superoxide dismutase presenting characteristic clinical features and Lewy body-like hyaline inclusions. *J Neurol Sci* 2004; **225**: 19–25.

26. Arisato T, Okubo R, Arata H *et al.* Clinical and pathological studies of familial amyotrophic lateral sclerosis (FALS) with SOD1 H46R mutation in large Japanese families. *Acta Neuropathol* 2003; **106**: 561–568.

Human Molecular Genetics, 2009, Vol. 18, No. 18 **3353–3364**
doi:10.1093/hmg/ddp275
Advance Access published on June 10, 2009

Truncation and pathogenic mutations facilitate the formation of intracellular aggregates of TDP-43

Takashi Nonaka[1,*], Fuyuki Kametani[1], Tetsuaki Arai[2], Haruhiko Akiyama[2] and Masato Hasegawa[1,*]

[1]Department of Molecular Neurobiology and [2]Department of Psychogeriatrics, Tokyo Institute of Psychiatry, Tokyo Metropolitan Organization for Medical Research, 2-1-8 Kamikitazawa, Setagaya-ku, Tokyo 156-8585, Japan

Received April 5, 2009; Revised May 27, 2009; Accepted June 8, 2009

TAR DNA binding protein of 43 kDa (TDP-43) is a major component of the ubiquitin-positive inclusions found in the brain of patients with frontotemporal lobar degeneration (FTLD-U) and amyotrophic lateral sclerosis (ALS). Here, we report that expression of TDP-43 C-terminal fragments as green fluorescent protein (GFP) fusions in SH-SY5Y cells results in the formation of abnormally phosphorylated and ubiquitinated inclusions that are similar to those found in FTLD-U and ALS. Co-expression of DsRed-tagged full-length TDP-43 with GFP-tagged C-terminal fragments of TDP-43 causes formation of cytoplasmic inclusions positive for both GFP and DsRed. Cells with GFP and DsRed positive inclusions lack normal nuclear staining for endogenous TDP-43. These results suggest that GFP-tagged C-terminal fragments of TDP-43 are bound not only to transfected DsRed-full-length TDP-43 but also to endogenous TDP-43. Endogenous TDP-43 may be recruited to cytoplasmic aggregates of TDP-43 C-terminal fragments, which results in the failure of its nuclear localization and function. Interestingly, expression of GFP-tagged TDP-43 C-terminal fragments harboring pathogenic mutations that cause ALS significantly enhances the formation of inclusions. We also identified cleavage sites of TDP-43 C-terminal fragments deposited in the FTLD-U brains using mass spectrometric analyses. We propose that generation and aggregation of phosphorylated C-terminal fragments of TDP-43 play a primary role in the formation of inclusions and resultant loss of normal TDP-43 localization, leading to neuronal degeneration in TDP-43 proteinopathy.

INTRODUCTION

Progressive neuronal loss and abnormal protein deposits as intracellular inclusions are neuropathological features of the majority of neurodegenerative disorders, as exemplified by tau in Alzheimer's disease (AD), alpha-synuclein in Parkinson's disease (PD) and expanded polyglutamine gene products in CAG repeat diseases. Conformational changes, post-translational modifications or subcellular mislocalization of these normally highly soluble proteins results in the formation of abnormal protein aggregates or inclusions. It is important to establish the molecular mechanisms through which these proteins are converted to abnormal aggregates in neurons or glial cells in order to understand the pathogenesis of these diseases and to develop evidence-based, fundamental therapies.

Frontotemporal lobar degeneration with ubiquitinated inclusions (FTLD-U) and amyotrophic lateral sclerosis (ALS) are well-known neurodegenerative disorders. FTLD is the second most common form of cortical dementia in the population below the age of 65 years (1). ALS is the most common of the motor neuron diseases, being characterized by progressive weakness and muscular wasting, resulting in death within a few years. Ubiquitin (Ub)-positive inclusions are found as a pathological hallmark in brains of FTLD-U and ALS patients, as well as in AD and PD, but the major component of these inclusions had remained unknown. TAR-DNA binding protein of 43 kDa (TDP-43) has been identified as a major protein component of Ub-positive inclusions in FTLD-U and ALS brains (2,3). In 2008, mutations in the TDP-43 gene were discovered in familial

*To whom correspondence should be addressed. Tel: +81 333045701; Fax: +81 333298035; Email: nonakat@prit.go.jp (T.N.)/masato@prit.go.jp (M.H.)

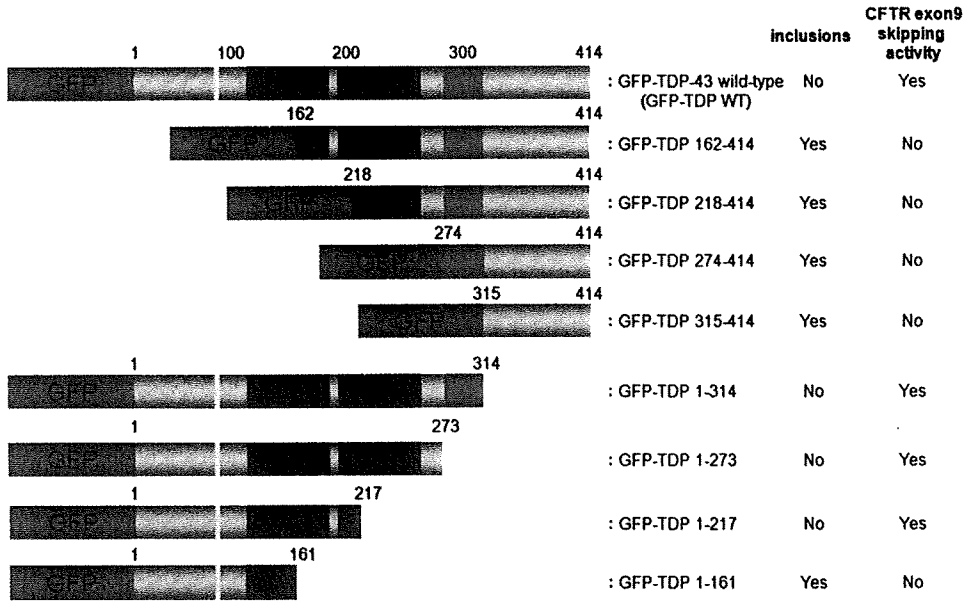

Figure 1. Schematic diagram of GFP-tagged N-terminal and C-terminal TDP-43 fragments. Green fluorescent protein (GFP), nuclear localization signal (NLS: 82–98 residues), two RNA-recognition motifs (RRM-1, 105–169 residues; RRM-2, 193–257 residues) and glycine-rich domain (274–314 residues) were colored green, yellow, blue and red, respectively. The formation of inclusions and the exon skipping ability of each fragment were reported on the right. The CFTR exon 9 skipping activity of these fragments were determined as shown in Fig. 5.

and sporadic cases of ALS (4–8), clearly indicating that abnormality of TDP-43 protein causes neurodegeneration. Very recently, it was also reported that two TDP-43 mutations were found in FTLD-MND patients (9). In previous genetic studies of familial ALS, superoxide dismutase 1 (SOD1) gene mutation was considered to be responsible for ~20% of cases (10,11). It has been reported, however, that TDP-43 is not deposited in spinal cords of familial ALS patients with SOD1 mutations (12,13). These observations suggest that the mechanisms of motor neuron degeneration caused by SOD1 mutations are different from those in sporadic ALS. TDP-43 is also a major component of skein-like inclusions seen in 100% of sporadic ALS cases (14). Thus, it is important to investigate the molecular mechanisms of TDP-43-mediated neurodegeneration in order to understand the pathogenesis and to develop effective treatments for sporadic ALS and other TDP-43 proteinopathies. One of the known biochemical features of TDP-43 deposited in FTLD-U and ALS brains is the presence of truncated TDP-43 fragments (2,3). Recently, using multiple anti-phosphorylated TDP-43 specific antibodies including pS409/410-specific antibodies, we have shown that 18–26 kDa C-terminal fragments of TDP-43 are major constituents of inclusions in FTLD-U and ALS brains (15).

In this study, we investigated the roles of fragmentation and pathogenic mutations of TDP-43 for the formation of Ub-positive inclusions in SH-SY5Y cells. Here we show that expression of TDP-43 C-terminal fragments results in the formation of cytoplasmic inclusions positive for antibodies to phosphorylated TDP-43 and Ub, and incorporation of newly synthesized endogenous full-length TDP-43 into cytoplasmic aggregates of the C-terminal fragments. Expression of fourteen pathogenic ALS mutations so far discovered in the TDP-43 gene shows a propensity to promote intracellular aggregation. Furthermore, using mass spectrometric analysis, we have successfully identified new cleavage sites of C-terminal fragments of TDP-43 deposited in FTLD-U brains.

RESULTS

Expression of TDP-43 fragments in SH-SY5Y cells

To examine whether C-terminal fragments of TDP-43 readily aggregate in neuronal cells, we expressed several kinds of N-terminal and C-terminal fragments of TDP-43 and full-length TDP-43 as GFP-fusions (Fig. 1). Confocal microscopic analysis showed that the fluorescence of GFP-tagged full-length TDP-43 (GFP-TDP WT) was mainly localized in the nuclei (Fig. 2B). This is consistent with the expression pattern of non-tagged wild-type TDP-43 (16), suggesting that the GFP tag did not alter the cellular localization of TDP-43.

When cells were transfected with GFP-TDP 162-414 or GFP-TDP 218-414, round or dot-like cytoplasmic structures with intense GFP fluorescence were found (Fig. 2C–F). These structures were positive for both anti-pS409/410 and anti-Ub antibodies (Fig. 2C–F). Cells expressing GFP-TDP 274–414 (Fig. 2G and H) and GFP-TDP 315–414 (Fig. 2I and J), on the other hand, showed diffuse GFP staining and pS409/410-positive but Ub-negative inclusion-like structures. We previously reported the presence of such pS409/410-positive and Ub-negative inclusions in the brains of FTLD-U and ALS cases (15). The expression of these all C-terminal fragments was found in cytoplasm by analyses using confocal microscopy (Fig. 2) and biochemical fractionation (Supplementary Material, Fig. S1A), because they lacks nuclear localization signal (16,17). Taken together, these results indicate that cytoplasmic expression of C-terminal

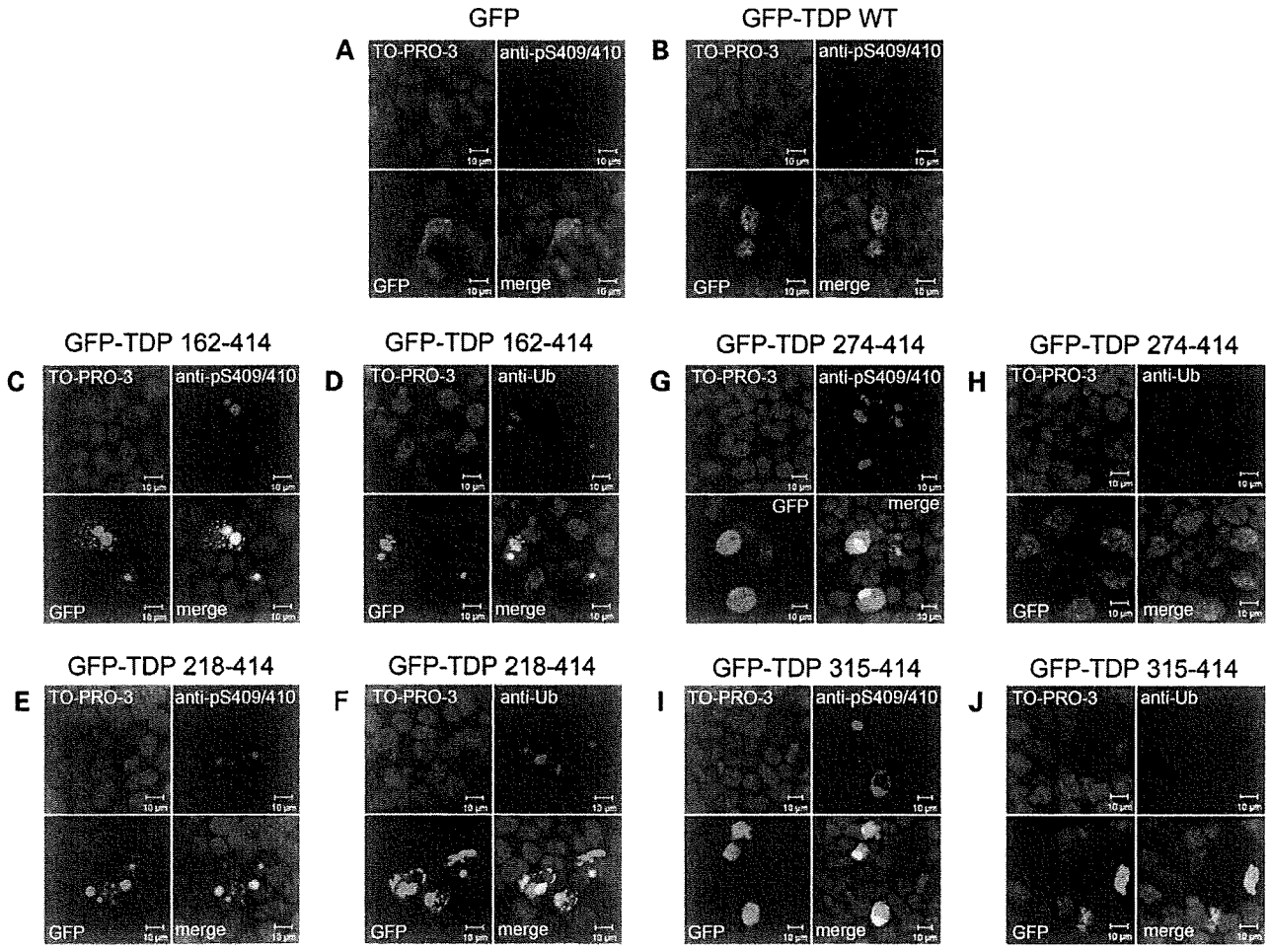

Figure 2. Expression of GFP-tagged C-terminal fragments of TDP-43 leads to aggregate formation in SH-SY5Y cells. SH-SY5Y cells 72 h post-transfection with GFP (**A**), GFP-tagged TDP-43 wild-type (GFP-TDP WT) (**B**), GFP-tagged fragments of residues 162–414 (GFP-TDP 162–414) (**C** and **D**), GFP-TDP 218–414 (**E** and **F**), GFP-TDP 274–414 (**G** and **H**) and GFP-TDP 315–414 (**I** and **J**) were stained with anti-pS409/410 (A, B, C, E, G, I) or anti-Ub (D, F, H, J). DNA was labeled with TO-PRO-3. Note that there are intracellular inclusion-like structures positive for both anti-Ub and anti-pS409/410 antibodies in cells expressing GFP-TDP 162–414 (C, D) and GFP-TDP 218–414 (E, F).

fragments of TDP-43 results in the formation of intracellular aggregates similar to those found in diseased brains.

N-terminal fragments of GFP-TDP-43 were also expressed in SH-SY5Y cells and analyzed using confocal microscopy and biochemical fractionation. As shown in Fig. 3A, irregularly shaped cytoplasmic structures with strong GFP fluorescence, which are partially positive for Ub, were observed in cells expressing GFP-TDP 1–161. Only a few aggregates positive for Ub were observed in cells transfected with GFP-TDP 1–217 (Fig. 3B). Since these fragments lack the epitope for anti-pS409/410, the phosphorylation state of these structures could not be determined by immunohistochemistry. None of the cells transfected with other N-terminal fragments had any Ub-positive inclusion-like structures (Fig. 3C and D). The results of biochemical fractionation showed that the amount of these N-terminal fragments was greater in the cytoplasm than in the nucleus, while that of GFP-TDP WT was greater in the nucleus than in the cytoplasm (Supplementary Material, Fig. S1A). These results suggest that truncations of TDP-43 C-terminal regions affect normal targeting of TDP-43 to nuclei. This observation is in good agreement with the previous report by Ayala *et al.* (18).

Since intracellular inclusion-like structures showed the highest-intensity GFP signals in Figs 2 and 3, they were able to be selectively detected by reducing the laser power at 488 nm. Quantitative analyses under such analytical conditions clearly indicated that significantly a larger number of intracellular aggregates were formed in cells expressing GFP-TDP 162–414, GFP-TDP 218–414 and GFP-TDP 1–161 than in cells expressing GFP-TDP WT (Fig. 3E).

Figure 4 shows the results of immunoblot analyses of cell lysates using anti-GFP, a commercially available phosphorylation-independent anti-TDP-43 (ProteinTech), and anti-pS409/410 antibodies. Anti-TDP-43 detected endogenous TDP-43 at 43 kDa, exogenous full-length TDP-43, all N-terminal fragments and GFP-TDP 162–414, but did not GFP-TDP 218–414, 274–414 and 315–414 (Fig. 4A and D). These results suggest that the epitopes of this antibody are located in the N-terminal region between 1 and 217 residues. Anti-GFP antibody stained all the exogenous TDP-43

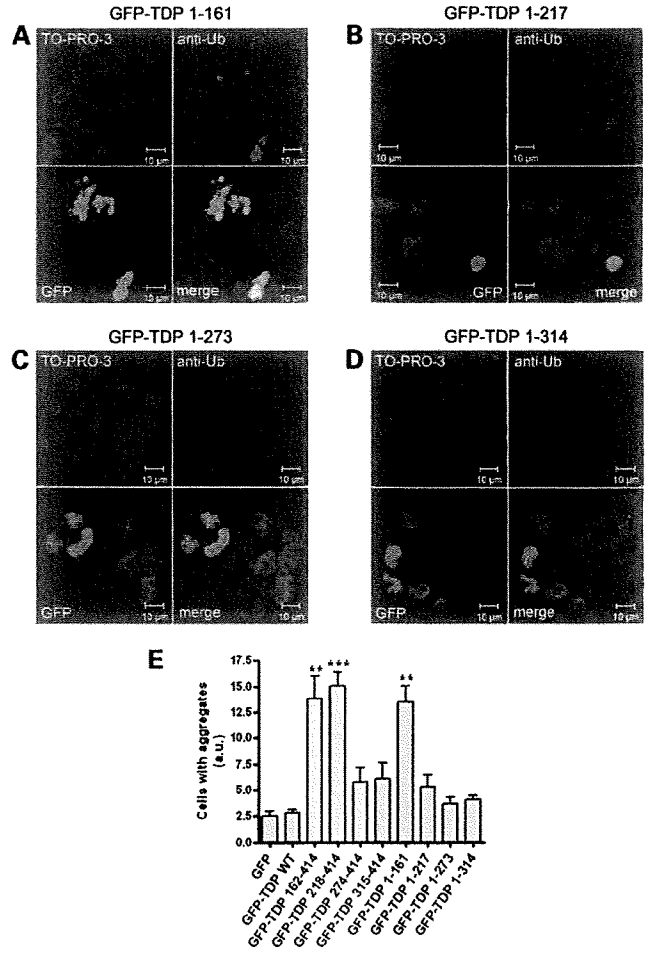

Figure 3. Expression of GFP-tagged N-terminal fragments of TDP-43 resulted in the formation of intracellular inclusions in SH-SY5Y cells. SH-SY5Y cells 72 h post-transfection with GFP-tagged fragments of 1–161 residues (GFP-TDP 1–161) (**A**), GFP-TDP 1–217 (**B**), GFP-TDP 1–273 (**C**) and GFP-TDP 1–314 (**D**) were stained with anti-Ub. DNA was labeled with TO-PRO-3. Note the characteristic inclusions detected with anti-Ub antibody in cells transfected with GFP-TDP 1–161. (**E**) The rates of cells including intracellular aggregates were calculated in arbitrary units. Fluorescence intensity within an area of ~800 × 800 μm was assessed by confocal microscopy. The intensity of GFP was calculated as a ratio to that of TO-PRO-3. Six areas per sample were measured ($n = 6$). Data are means ± SEM. $^{**}P < 0.01$; $^{***}P < 0.001$ by Student's *t*-test against the value of GFP-TDP WT.

(Fig. 4B and E). In these immunoblot analyses, we used the intensity of the bands of endogenous TDP-43 (arrows in Fig. 4A and D) as a loading control. While the amounts of exogenous protein are nearly constant, that of 1–161 is relatively low and those of 274–414 and 315–414 relatively high. Nevertheless, such variability does not affect the occurrence or absence of inclusion formation (Fig. 1). Endogenous and exogenous full-length TDP-43 (GFP-TDP WT) were detected mostly in TS-, TX- and Sar-soluble fractions, and were negative for anti-pS409/410 (Fig. 4).

Although GFP-TDP 162–414 was also detected in TS-, TX- and Sar-soluble fractions with anti-TDP-43 and anti-GFP, a slightly higher-molecular-weight band (~60 kDa, black arrowhead in Fig. 4C) was detected in Sar-soluble and insoluble fractions with anti-pS409/410. A similar band was only weakly detected with anti-TDP-43 (black arrowhead in Fig. 4A), and was negative to anti-GFP antibody. These results confirmed our previous reports that our anti-pS409/410 is specific to and is more sensitive in detecting abnormally accumulated TDP-43 than phosphorylation-independent antibodies such as anti-TDP-43 (ProteinTech) (15,16,19). Anti-GFP used here seems to be less sensitive in immunoblot. Anti-GFP may also be affected by possible structural changes during aggregates formation when applied to the Sarkosyl insoluble fraction. GFP-TDP 218–414 was mainly detected in Sar-soluble and -insoluble fractions with anti-GFP (Fig. 4B), and a slightly higher-molecular-weight band at 52 kDa (white arrowhead in Fig. 4C) and smears were visualized in the Sar-soluble and -insoluble fractions with anti-pS409/410. Similarly, pS409/410-positive bands were detected in the Sar-soluble and insoluble fractions of cell lysates expressing GFP-TDP 274–414 or GFP-TDP 315–414 (black-lined arrowhead for GFP-TDP-274–414; white-lined arrowhead for GFP-TDP 315–414 in Fig. 4C), although no abnormal band pattern was detected with anti-TDP-43 or anti-GFP.

The N-terminal fragments, including GFP-TDP 1–314, GFP-TDP 1–273 and GFP-TDP 1–217, were detected mainly in the TS- and TX-soluble fractions, together with GFP-TDP WT and endogenous TDP-43 (Fig. 4D and E). However, GFP-TDP 1–161, the shortest N-terminal fragment, was detected only in the Sar-soluble fraction (black-lined arrowheads in Fig. 4D and E), which is consistent with the inclusion formation observed in cells expressing this fragment, as shown in Fig. 3A.

Loss of function and intracellular accumulation of TDP-43 fragments

TDP-43 has been reported to regulate the alternative splicing of exon 9 of cystic fibrosis transmembrane conductance regulator (CFTR) transcripts (20). TDP-43 is capable of binding to a (UG)nUm element in CFTR intron 8 near its junction with exon 9. Through this binding, TDP-43 enhances the exon skipping of exon 9 during CFTR splicing. To evaluate the functional significance of TDP-43 fragments used in this study, we performed CFTR exon 9 skipping assay (16). We co-transfected the expression plasmid of TDP-43 wild-type or fragments with the reporter plasmid pSPL3-CFTR9 (including a TG11T7 polymorphic locus) (16) into SH-SY5Y cells. The transcripts with and without the CFTR exon 9 insert are expected to be 360 and 177 bp long, respectively (16), and these were analyzed by RT–PCR. As shown in Fig. 5, mRNA from cells transfected with empty vector pEGFP gave only one RT–PCR band of 360 bp, while that from cells transfected with TDP-43 wild-type gave two RT–PCR bands, 360 and 177 bp, showing that skipping of CFTR exon 9 was increased by expression of GFP-TDP WT. We also confirmed that the GFP portion did not affect the CFTR exon skipping activity of TDP-43. All mRNAs from cells co-transfected with the C-terminal fragments showed one RT–PCR band of 360 bp (Fig. 5A). Of the four mRNAs from cells co-transfected with the N-terminal fragments, mRNA from GFP-TDP 1-161 showed a band of 360 bp, while the others showed two bands of 360 and 177 bp (Fig. 5B). These results indicate that the fragments without

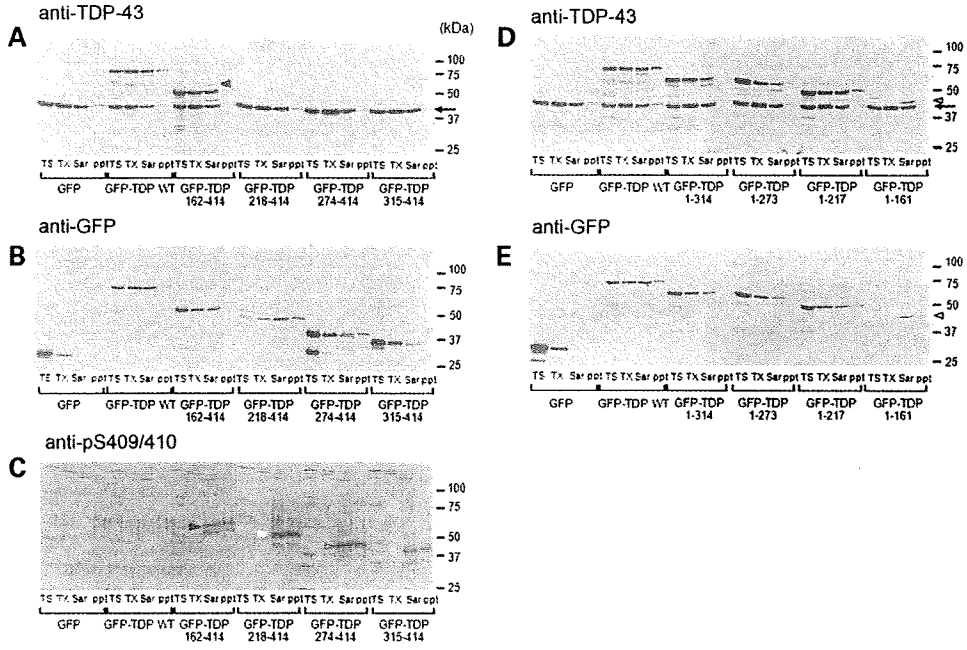

Figure 4. Immunoblot analyses of inclusions composed of GFP-tagged N-terminal and C-terminal fragments of TDP-43. SH-SY5Y cells, 72 h post-transfection with GFP alone or GFP-fused TDP-43 fragments, were sequentially extracted with Tris-saline (TS), 1% Triton X-100 (TX) and 1% Sarkosyl (Sar), and the supernatants and the Sarkosyl-insoluble pellets (ppt) were subjected to SDS–PAGE. Bands were transferred to PVDF membrane and probed with anti-TDP-43 antibody (**A** and **D**), anti-GFP antibody (**B** and **E**) and anti-pS409/410 antibody (**C**). The arrow indicated the band of endogenous TDP-43. Note that bands of pS409/410-positive C-terminal fragments were detected in Sarkosyl-soluble or -insoluble fractions of cells expressing GFP-TDP 162–414 (black arrowhead in C), GFP-TDP 218–414 (white arrowhead in C), GFP-TDP 274–414 (black-lined arrowhead in C) and GFP-TDP 315–414 (white-lined arrowhead in C), and that N-terminal fragment of GFP-TDP 1–161 was recovered in TX-insoluble fractions (black-lined arrowhead in D and E).

the entire RRM-1 motif do not have exon skipping activity, while the wild-type and fragments with the RRM-1 motif have the activity (Figs 1 and 5). These results are in good agreement with the observation by Buratti and Baralle (21) that the RRM-1 domain is necessary for binding with RNA. It is noteworthy that all the TDP-43 fragments which form intracellular aggregates lack exon skipping activity.

Expression of TDP-43 C-terminal fragment facilitates aggregation of full-length TDP-43 in SH-SY5Y cells

To test whether C-terminal fragments of TDP-43 interact with full-length TDP-43, C-terminal fragments of GFP-TDP-43 or full-length GFP-TDP-43 was co-expressed with full-length DsRed-fused TDP-43 (DsRed-TDP-43) in SH-SY5Y cells. Immunoprecipitation experiments of cell lysates using agarose conjugated anti-GFP followed by immunoblotting with anti-RFP or anti-TDP-43 showed that GFP-TDP-43 C-terminal fragments as well as full-length GFP-TDP-43 were bound to full-length DsRed-TDP-43 (Fig. 6). Full-length GFP-TDP-43 was found to more strongly interact with DsRed-TDP-43 than any other C-terminal fragments of GFP-TDP-43. The experiments also showed a weak but notable interaction between endogenous TDP-43 and full-length GFP-TDP-43 or C-terminal fragments of GFP-TDP-43. These results suggest that both full-length GFP-TDP-43 and its C-terminal fragments interact not only with full-length DsRed-TDP-43 but also with endogenous TDP-43 in SH-SY5Y cells.

To monitor the intracellular interaction between endogenous TDP-43 and C-terminal fragments of GFP-TDP-43, SH-SY5Y cells were transfected with GFP-TDP 162–414 or GFP-TDP 218–414 and analyzed by confocal microscopy. Immunostaining using anti-TDP-43 showed that full-length GFP-TDP-43 was co-localized with endogenous TDP-43 in nuclei (Fig. 7A). We observed that GFP signals from cytoplasmic inclusions of GFP-TDP 162–414 or GFP-TDP 218–414 were overlapped with immunoreactivities of anti-TDP-43. Furthermore, immunoreactivities of anti-TDP-43 were almost eliminated from the nuclei of these cells (Fig. 7B and C). When full-length GFP-TDP-43 was co-expressed with full-length DsRed-TDP-43, both proteins were found to be localized in nuclei with no formation of inclusion-like structures (Fig. 7D). In contrast, round cytoplasmic inclusions with both GFP and DsRed signals appeared when GFP-TDP 162–414 (Fig. 7E) or GFP-TDP 218–414 (Fig. 7F) was co-expressed with full-length DsRed-TDP-43. These results indicate that endogenous TDP-43 or exogenous full-length DsRed-TDP-43 is trapped into cytoplasmic inclusions formed by GFP-TDP 162–414 or GFP-TDP 218–414, which is consistent with the results of immunoprecipitation experiments shown in Fig. 6.

Effects of pathogenic mutations on aggregation of TDP-43

Then, we tested the effect of mutations of the TDP-43 gene found in familial and sporadic ALS cases on the intracellular aggregates of C-terminal fragments of GFP-TDP-43 (GFP-TDP 162–414). GFP-TDP 162–414 with or without mutations was expressed in SH-SY5Y cells, which were then analyzed by immunoblot and confocal microscopy. We first confirmed almost same expression levels of all exogenous

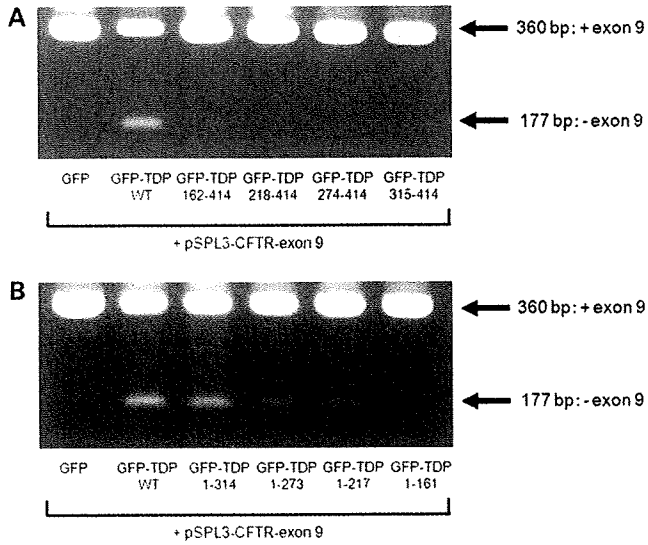

Figure 5. CFTR exon 9 skipping assay of GFP-tagged TDP-43 fragments. (**A** and **B**) Gel electrophoresis of RT–PCR products of RNA from transfected cos-7 cells. The RNAs from cos-7 cells, co-transfected with the reporter plasmid pSPL3-CFTR exon 9 (TG11T7) plus pEGFP-TDP-43 expression vectors, were used as templates for RT–PCR analysis. The products were analyzed by electrophoresis in 1.5% agarose gel.

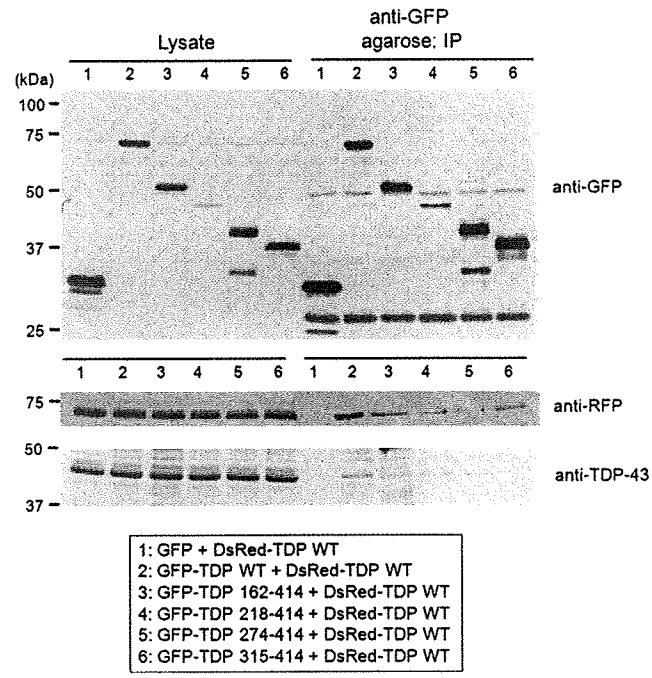

Figure 6. Full-length GFP-TDP-43 and its C-terminal fragments interact not only with full-length DsRed-TDP-43 but also with endogenous TDP-43. SH-SY5Y cells were transfected with pDsRed-TDP-43 wild-type (DsRed-TDP WT) and pEGFP-C1 (GFP; lane 1), pEGFP-TDP-43 WT (GFP-TDP WT; lane 2), pEGFP-TDP 162–414 (GFP-TDP 162–414; lane 3), pEGFP-TDP 218–414 (GFP-TDP 218–414; lane 4), pEGFP-TDP 274–414 (GFP-TDP 274–414; lane 5) or pEGFP-TDP 315–414 (GFP-TDP 315–414; lane 6), for 3 days, and analyzed by immunoprecipitation. Cell lysates (total protein: ~100 μg) was recovered and subjected to IP with agarose conjugated anti-GFP (~5 μg of anti-GFP, MBL). Bounds proteins were eluted from the beads with SDS sample buffer. Each sample (~5 μg of lysates and ~1/5 aliquots of IP fraction) was separated by 10% SDS–PAGE and immunoblotted with anti-GFP antibody, anti-RFP antibody and anti-TDP-43 antibody.

GFP-TDP 162–414 with or without mutations by immunoblot analysis with anti-TDP-43 (Fig. S2). Figure 8 showed that all 14 mutant GFP-TDP 162–414 formed more intracellular aggregates than wild-type GFP-TDP 162–414. Of these mutations, the number of cells with aggregates was significantly higher in GFP-TDP 162–414 with D169G, G294A, Q331K, M337V, Q343R, N390D and N390S, when compared with the wild-type GFP-TDP 162–414 (Fig. 8B).

When full-length TDP-43 with or without GFP fusion was expressed in cells, we could not find any significant difference in the number of cells with aggregates between wild-type and all mutants (data not shown). Furthermore, there was no significant difference in the generation of TDP-43 fragments (Supplementary Material, Fig. S3) or exon skipping activity of CFTR exon 9 between wild-type full-length TDP-43 and mutated full-length TDP-43 (data not shown).

Identification of the cleavage sites of N-terminally truncated TDP-43 fragments in FTLD-U brains

To identify the cleavage sites of the C-terminal fragments of TDP-43 accumulated in brains of FTLD-U patients, we performed protein chemical analyses of the major fragments of 18–26 kDa in the Sarkosyl-insoluble fraction (Fig. 9A). Mass spectra analysis of tryptic digests of these fragments identified two typical tryptic peptides, (K)GISVHISNAEPKHNSNR (residues 252–268) and (R)FGGNPGGFG NQGGFGNSR (residues 276–293), and two unusual tryptic peptides, (M)DVFIPKPFR (residues 219–227) (Fig. 9B) and (E)DLIIK (residues 247–251) (Fig. 9C). N-termini of the latter two peptides are not produced by trypsin, because this enzyme cannot cleave Met218-Asp219 and Glu246-Asp247 bonds. These results suggest that these peptides are N-terminal parts of C-terminal fragments of TDP-43, and that the major C-terminal fragments deposited in FTLD-U brains are produced by cleavage between Met218-Asp219 or Glu246-Asp247.

To characterize these C-terminal fragments of TDP-43 deposited in FTLD-U brains with regards to intracellular aggregates formation, phosphorylation, and CFTR exon 9 splicing activity, GFP-TDP 219–414 and GFP-TDP 247–414 were constructed and expressed in SH-SY5Y cells for 3 days. These cells were analyzed using confocal microscopy, immunoblot and CFTR exon 9 skipping assay. As shown in Fig. 10A, round cytoplasmic inclusions with GFP fluorescence were clearly observed in cells expressing GFP-TDP 219–414 or GFP-TDP 247–414. These were also positive for anti-pS409/410 and anti-Ub. In immunoblot analyses, GFP-TDP 219–414 and GFP-TDP 247–414 were detected in Sar-soluble and insoluble fractions with anti-pS409/410 (Fig. 10B). These results suggest that these C-terminal fragments have high propensity to aggregate in cells, which is in good agreement with above results obtained from cells expressing other C-terminal fragments (e.g. GFP-TDP 218–414). Furthermore, expression of each C-terminal fragment resulted in a decrease in exon 9 skipping activity relative to GFP-TDP wild-type, as shown in Fig. 10C. We also found that overexpression of these C-terminal fragments led to a slight but

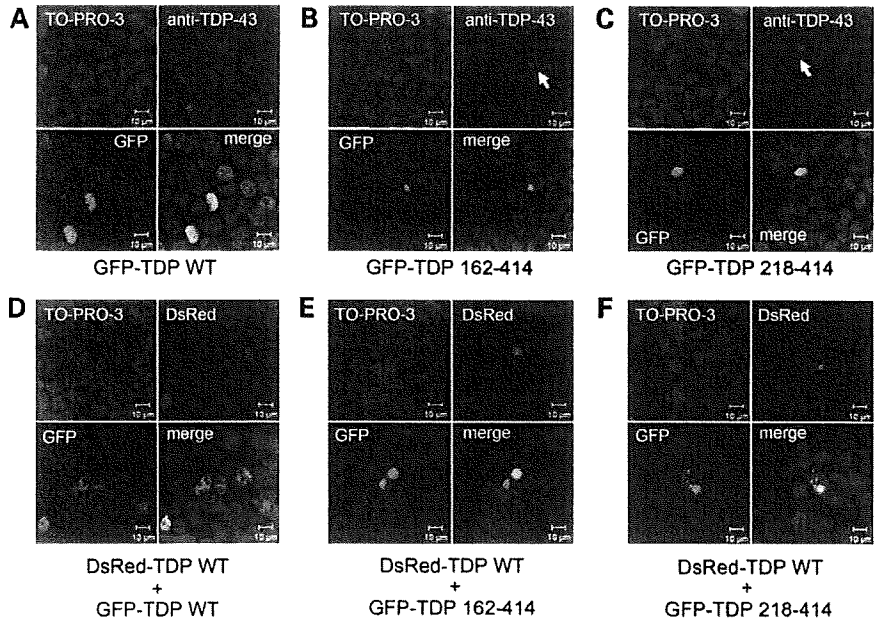

Figure 7. Co-expression of both DsRed-TDP-43 wild-type and GFP-TDP-43 wild-type or its C-terminal fragments. SH-SY5Y cells were transfected with pEGFP-TDP-43 wild-type (GFP-TDP WT), pEGFP-TDP 162–414 (GFP-TDP 162–414), pEGFP-TDP 218–414 (GFP-TDP 218–414) with (**D**–**F**) or without pDsRed-TDP-43 WT (**A**–**C**) for 3 days, and analyzed by confocal microscopy. Endogenous TDP-43 was stained by anti-TDP-43 antibody (ProteinTech) in (A–C). DNA was stained with TO-PRO-3. The threshold gain level of laser power (543 nm for detection of DsRed) was adjusted so that the signals did not overlap. Immunoreactivities of anti-TDP-43 were almost eliminated from the nuclei of cells with inclusions of GFP-TDP 162–414 (arrow in B) and GFP-TDP 218–414 (arrow in C).

significant increase in CFTR exon 9 inclusion (Fig. 10C, lower panel). This result suggests that endogenous TDP-43 was trapped with these aberrant C-terminal fragments, resulting a loss of exon 9 exclusion activity by endogenous TDP-43.

DISCUSSION

In this work, we showed that expression of C-terminal and N-terminal fragments of TDP-43 as GFP fusions resulted in the formation of phosphorylated and ubiquitinated aggregates in cultured cells. We first tried to express non-tagged C-terminal TDP-43 fragment (residues 162–414 or 218–414) in SH-SY5Y cells, but without success (data not shown). We then constructed plasmids encoding GFP-tagged N-terminal and C-terminal fragments of TDP-43, as shown in Fig. 1. The C-terminal fragments were significantly more prone to aggregate than full-length TDP-43. These aggregated C-terminal fragments were phosphorylated at Ser409 and Ser410, and were recovered in the TX-insoluble and Sar-soluble as well as Sar-insoluble fractions. These features are consistent with our previous findings, which showed that phosphorylated C-terminal fragments of TDP-43 were the major component of Sar-insoluble TDP-43 in the FTLD-U and ALS brains (15).

Recently, Johnson *et al.* (22) reported a yeast TDP-43 proteinopathy model. They found that RRM-2 and a C-terminal region (188–414 residues) are required for TDP-43 to form toxic aggregates. The fact that the highest propensity to aggregate was seen with GFP-TDP 162–414 and GFP-TDP 218–414 in the present study is consistent with their observations. However, the formation of pS409/410-positive inclusion-like structures in cells expressing C-terminal fragments without RRM2 (GFP-TDP 274–414 and 315–414), and the lack of striking cell death in cells expressing any GFP-tagged TDP-43 fragments (data not shown), differ from their findings. Furthermore, we could not detect intracellular aggregates formed by full-length GFP-TDP-43 in this study. One of the reasons for such discrepancies may be the differences between cultured neuronal cells and yeast.

We also found that one of the N-terminal fragments of TDP-43, GFP-TDP 1-161 were also prone to aggregate in cultured cells. This fragment was recovered in the TX-insoluble and Sar-soluble fraction. Previous reports indicated that lower-molecular-weight bands were present in the Sar-insoluble fractions of FTLD-U cases using the anti-TDP-43 (ProteinTech) (2,3,23). In this study, we established that this antibody recognizes the epitopes in the N-terminal portion between the residues 1 and 217 but not the C-terminal portion. Therefore, N-terminal fragments of TDP-43 may be present in the Sar-insoluble fraction of FTLD-U samples. It is noteworthy, therefore, that the expression of N-terminal TDP-43 fragments, as well as C-terminal fragments, could cause the formation of cytoplasmic aggregates in cultured cells.

The results of co-expression experiments using GFP-TDP 162–414 or GFP-TDP 218–414 and full-length DsRed-TDP-43 (Fig. 7) are consistent with the notion that cytoplasmic aggregates of C-terminal fragments of TDP-43 initially formed recruit newly synthesized full-length TDP-43 monomer and stay it in cytoplasm, resulting in depleting normal nuclear TDP-43. This may explain why normal TDP-43 staining is cleared in nuclei of diseased neurons containing cytoplasmic TDP-43 aggregates. Such mislocalization of full-length TDP-43 may induce neuronal dysfunction due to loss of

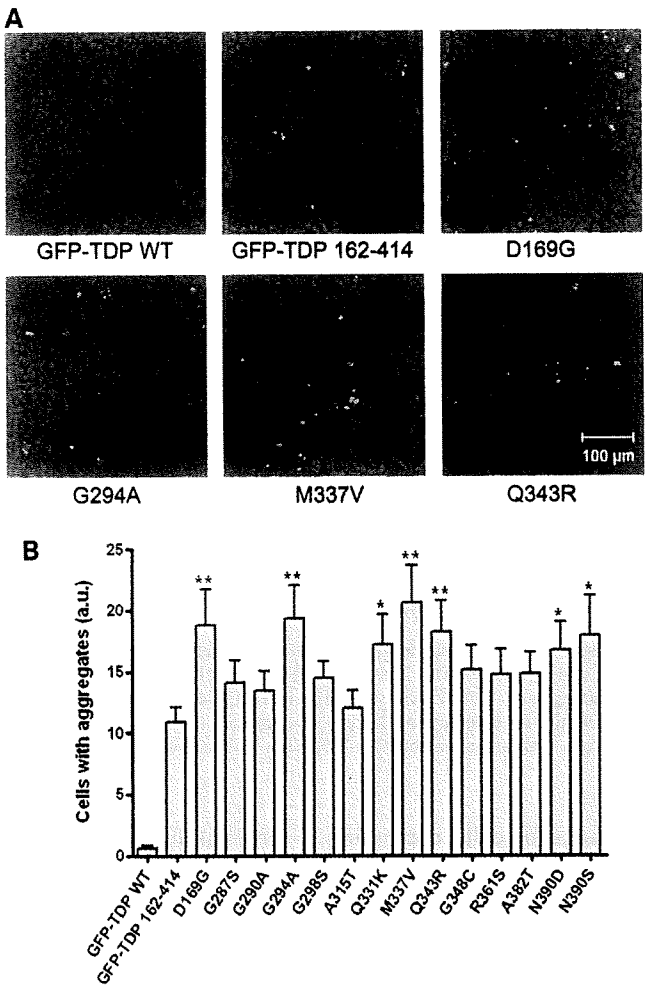

Figure 8. The effects of pathogenic mutations found in familial and sporadic ALS on intracellular accumulations of GFP-tagged TDP-43 C-terminal fragment. SH-SY5Y cells were transfected with GFP-TDP-43 wild-type (GFP-TDP WT), GFP-TDP 162-414 or each of 14 mutants (D169G, G287S, G290A, G294A, G298S, A315T, Q331K, M337V, Q343R, G348C, R361S, A382T, N390D and N390S) for 3 days, fixed and analyzed by confocal microscopy. DNA was stained with TO-PRO-3. (**A**) Images from cells transfected with GFP-TDP WT, GFP-TDP 162–414, GFP-TDP 162–414 with D169G (D169G), G294A (G294A), M337V (M337V) and Q343R (Q343R) were shown. (**B**) The rates of cells including intracellular aggregates were calculated in arbitrary units. Fluorescence intensity within an area of ~800 × 800 μm was assessed by confocal microscopy. The intensity of GFP was calculated as a ratio to that of TO-PRO-3. More than eight areas per sample were measured ($n = 8–16$). Data are means ± SEM. $^*P < 0.05$; $^{**}P < 0.01$ by Student's *t*-test against the value of GFP-TDP 162–414.

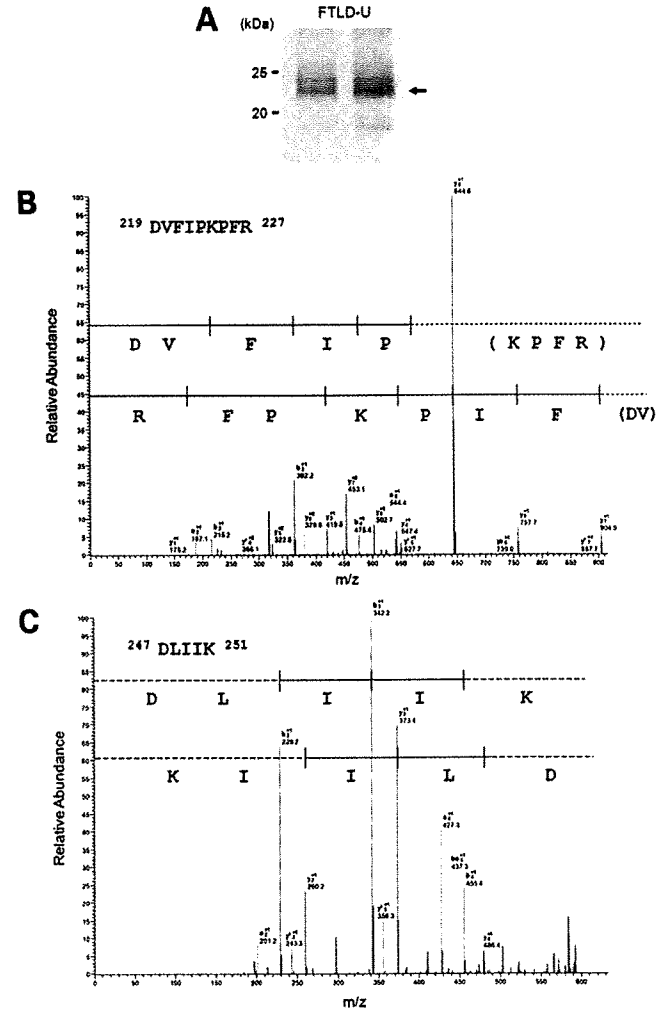

Figure 9. Identification of the cleavage site of TDP-43 C-terminal fragments deposited in FTLD-U brains. (**A**) C-terminal fragments of TDP-43 deposited in FTLD-U brains were detected with anti-pS409/410 (15). The pS409/410-positive ~23 kDa bands (an arrow) were dissected and digested in-gel with trypsin. (**B** and **C**) Product ion spectra of a mass signal $(M+2H)^{2+}$ of m/z 560.55 (B) and m/z 601.71 (C) from tryptic digests of urea-soluble C-terminal fragment of TDP-43 from FTLD-U brains. These spectra show the b and y ion series, identifying the peptide, DVFIPKPFR (residues 219–227) and DLIIK (residues 247–251), respectively. Vertical bars denote consecutive mass signals in b and y series.

physiological functions of TDP-43 in nuclei (3,17). In this study, we showed that expression of aberrant C-terminal fragment (GFP-TDP 219–414 or 247–414) resulted in decreased activity of CFTR exon 9 exclusion by endogenous TDP-43 due to its mislocalization in cytoplasm. It is also noteworthy that exogenously expressed full-length TDP-43 binds to each other, and the interaction between full-length TDP-43 is stronger than that between C-terminal fragments and full-length TDP-43. These results suggest that N-terminal portion may be essential for an inter-TDP-43 binding, which may contribute to its structural stability.

Interestingly, all TDP-43 fragments which form cytoplasmic aggregates lack CFTR exon 9 skipping activity (Figs 1 and 5). It was reported that the entire RRM-1 domain and C-terminal glycine-rich domain are required for CFTR exon 9 skipping (21,24–26). TDP-43 is considered to bind to hnRNP A/B through this domain (24). In our hands, all C-terminal fragments in this study lack skipping activity of CFTR exon 9, although these fragments retain the glycin-rich domain. Absence of RRM-1 or formation of cytoplasmic aggregates or both might impair the physiological functions of TDP-43, leading to cellular dysfunction and neurodegeneration. Further studies are needed to examine whether or not cellular function(s) (proliferation, differentiation, etc.) are affected in cells expressing TDP-43 fragments without the RRM-1 or glycine-rich domain or both.

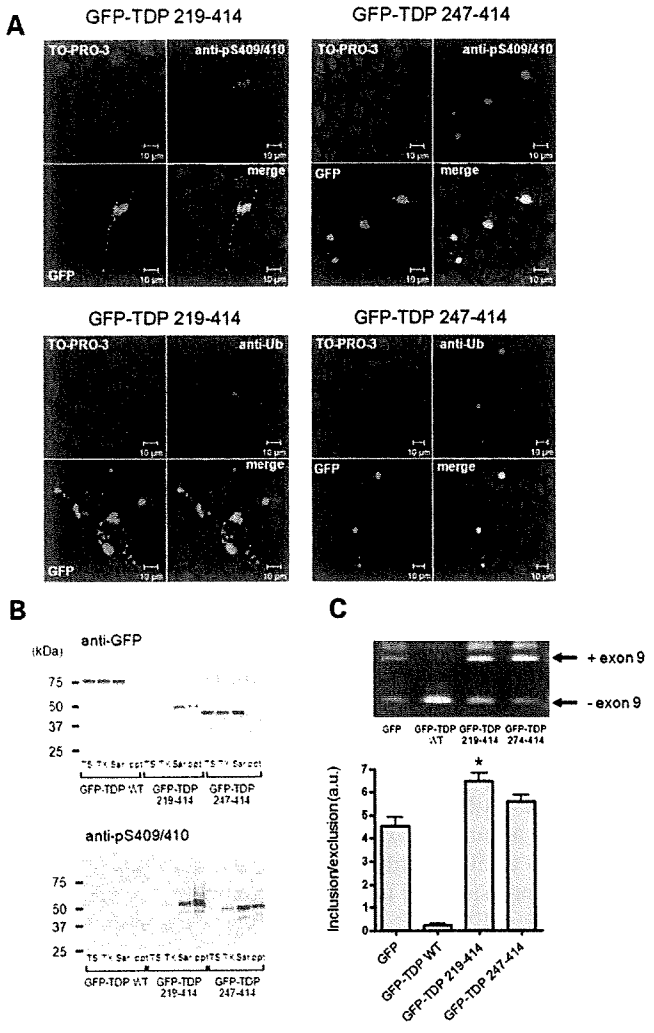

Figure 10. Pathological characterization of C-terminal fragments of TDP-43 identified in FTLD-U brains. (**A**) Confocal microscopic analyses of cells expressing GFP-TDP 219–414 (left) and GFP-TDP 247–414 (right). SH-SY5Y cells 72 h post-transfection with GFP-TDP 219–414 and GFP-TDP 247–414 were stained with anti-pS409/410 (upper) and anti-Ub (lower). (**B**) Immunoblot analyses of cells expressing GFP-TDP 219–414 and GFP-TDP 247–414. SH-SY5Y cells, 72 h post-transfection, were sequentially extracted with Tris-saline (TS), 1% Triton X-100 (TX) and 1% Sarkosyl (Sar), and the supernatants and the Sarkosyl-insoluble pellets (ppt) were subjected to SDS–PAGE. Bands were transferred to PVDF membrane and probed with anti-GFP antibody and anti-pS409/410 antibody. (**C**) CFTR exon 9 splicing assay. Gel electrophoresis of RT–PCR products of RNA from transfected cos-7 cells. The RNAs from cos-7 cells, co-transfected with the reporter plasmid pSPL3-CFTR exon 9 (TG13T5) plus pEGFP-TDP-43 expression vectors, were used as templates for RT–PCR analysis. The products were analyzed by electrophoresis in 1.5% agarose gel. The lower panel shows quantitative analyses of the ratio of CFTR exon 9 inclusion/exclusion. The intensity of each band was analysed using the Image J software. Data ($n = 4$) are means ± SEM. $^*P < 0.05$ by Student's *t*-test against the value of GFP.

Several groups have recently reported increased accumulation of TDP-43 fragments in the brain homogenates (8) and cultured cells (5,6) in some of the pathogenic mutations in ALS. The major component of abnormally accumulated TDP-43 is the C-terminal fragments in all TDP-43 proteinopathy (15,23). In this study, however, immunoblot analyses using a commercial TDP-43 antibody and our C-terminal 405–414 antibody (15,19) failed to show any significant differences in the generation of fragments of TDP-43 with or without various mutations (Supplementary Material, Fig. S3). The results of this study provide evidence, for the first time, that all 14 mutations tested consistently enhance aggregation of TDP-43 if they are present in the C-terminal fragments. We examined the effects of TDP-43 mutations on aggregates formation of both GFP-TDP 162–414 and GFP-TDP 218–414. We found that mutations significantly facilitate the formation of cytoplasmic inclusions of GFP-TDP 162–414, but not GFP-TDP 218–414 (data not shown). In this study, GFP-TDP 218–414 was found to be most prone to aggregate in SH-SY5Y cells. Thus, it seems likely that the high propensity to aggregate formation of GFP-TDP 218–414 may mask mutation effects on aggregates formation of GFP-TDP 218–414. So, we speculate that mutation effects were significantly detected in the experiments using GFP-TDP 162–414 which was less prone to form cytoplasmic inclusions than GFP-TDP 218–414. It seems reasonable to speculate that pathogenic mutations and N-terminal truncation synergistically promote abnormal accumulation of TDP-43. Failure to form aggregates in cells that express mutated full length TDP-43 suggests that the cell culture models recapitulate *in vivo* diseases only partially and that such models need N-terminal truncation of TDP-43 as a prerequisite for the mutation effect.

Igaz *et al.* (27) reported the cleavage site at Arg 208 in a pathological TDP-43 C-terminal fragment from FTLD-U brains and inclusion formation in cultured cells expressing resultant C-terminal fragment (residues 208–414). In the present study, by mass spectrometric analysis of the sarkosyl-insoluble fraction extracted from the FTLD-U brains, we newly identified two C-terminal fragments generated by N-terminal truncation at Asp219 and Asp247 of TDP-43 (196 and 168 amino acids, respectively). It should be noted that of these, the fragment cleaved at Asp219 (residues 219–414) is almost identical to TDP 218–414 employed in this study, which we found to be the most prone to aggregate in SH-SY5Y cells. We also confirmed that phosphorylated and ubiquitinated cytoplasmic inclusions were formed in cells expressing GFP-TDP 219–414 or GFP-TDP 247–414. Thus, the generation of aggregation-prone fragments of TDP-43 may play an important role for pathological process of TDP-43 proteinopathy. The N-termini of both identified peptides were Asp residue, suggesting that the protease(s) responsible for the cleavage may show specificity for the N-terminal side of Asp residues. Regarding the protease to degrade TDP-43, Zhang *et al.* (28) previously reported the occurrence of caspase cleavage of TDP-43 in cultured cells by the knockdown of progranulin gene. Furthermore, they recently reported the formation of intracellular inclusions immunopositive for phosphorylated TDP-43 and ubiquitin in cells expressing the GFP-tagged C-terminal fragment of TDP-43 (residues 220–414), which is expected to be generated by caspase cleavage (29). In the present study, however, we did not detect VFIPKPFR (residues 220–227), which is predicted to be produced by trypsin digestion of caspase-cleaved TDP-43, in the sarkosyl-insoluble fraction from the FTLD-U brains. These results suggest that caspase may not be the responsible enzyme for generation of

C-terminal fragments of TDP-43 in human brains. Since several abnormal fragments of 18–26 kDa were detected in FTLD-U and ALS with the antibodies to C-terminal region of TDP-43 like anti-pS409/410 (15, 19, 23), it seems reasonable to speculate the presence of the multiple cleavage sites in the middle of TDP-43. Thus, there may be other fragments, the N-termini of which have yet to be identified, and its responsible proteases. Further investigation of the degradation mechanism of TDP-43 might be needed to elucidate the pathogenesis of TDP-43 proteinopathy.

Our findings here provide further support for the idea that accumulation of fragmented TDP-43 plays an important role in TDP-43 proteinopathy. Our cellular models are expected to be useful tools to investigate the pathogenesis of TDP-43 proteinopathy, since they show pathological and biochemical characteristics similar to those of inclusions found in brains of patients, in terms of size, abnormal phosphorylation and ubiquitination.

MATERIALS AND METHODS

Construction of plasmids

To construct N-terminally green fluorescent protein (GFP)- and DsRed-fused TDP-43, a cDNA encoding full-length TDP-43 was amplified from pcDNA3-TDP-43 using the following primers: GFP/DsRed-forward, 5′-CCGCTCGAGCTA TGTCTGAATATATTCGGGTAACCGAA-3′; GFP/DsRed-reverse, 5′-CGGGATCCCTACATTCCCCAGCCAGAAG-3′. The amplified fragment was digested with *Xho*I/*Bam*HI and was cloned into the same cleavage sites of the pEGFP-C1 vector (Clontech) and pDsRed-Monomer-C1 vector (Clontech), respectively. For the construction of GFP-tagged TDP-43 fragments, each fragment was amplified by PCR using the following primers: for GFP-tagged TDP-43 fragment of residues 162–414 (GFP-TDP 162–414), forward, 5′-CC GCTCGAGCTATGTCACAGCGACATATGA-3′ and GFP/DsRed-reverse; for GFP-TDP 218–414, forward, 5′-CCGCT CGAGCTATGGATGTCTTCATCCCCA-3′ and GFP/DsRed-reverse; for GFP-TDP 219–414, forward, 5′-CCGCTCGAGCT GATGTCTTCATCCCCAAGCC-3′ and GFP/DsRed-reverse; for GFP-TDP 247–414, forward, 5′-CCGCTCGAGCT GACTTGATCATTAAAGGAAT-3′ and GFP/DsRed-reverse; for GFP-TDP 274–414, forward, 5′-CCGCTCGAGCTGGAAGATTTGGTGGTAATCCA-3′ and GFP/DsRed-reverse; for GFP-TDP 315–414, forward, 5′-CCGCTCGAGCTGCGTTCAGCATTAATCCAGCCAT-3′ and GFP/DsRed-reverse; for GFP-TDP 1–161, GFP/DsRed-forward and reverse, 5′-CGGGATCCCTATACTTTCACTT GTGTTT-3′; for GFP-TDP 1–217, GFP/DsRed-forward and reverse, 5′-CGGGATCCCTACACATCCCCGTACTGAG-3′; for GFP-TDP 1–273, GFP/DsRed-forward and reverse, 5′-CGGGATCCCTAACTTCTTTCTAACTGTCTATTGCT-3′; for GFP-TDP 1–314, GFP/DsRed-forward and reverse, 5′-CG GGATCCCTAACCAAAGTTCATCCCACCACCCAT-3′. The resulting products were digested with *Xho*I/*Bam*HI and were cloned into the same cleavage sites of the pEGFP-C1 vector (Clontech). Site-directed mutagenesis of GFP-tagged or non-tagged full-length TDP-43 and GFP-tagged C-terminal fragment (GFP-TDP 162–414) was carried out to substitute Asp169 to Gly (D169G), Gly287 to Ser (G287S), Gly290 to Ala (G290A), Gly294 to Ala (G294A), Gly298 to Ser (G298S), Ala315 to Thr (A315T), Gln331 to Lys (Q331K), Met337 to Val (M337V), Gln343 to Arg (Q343R), Gly348 to Cys (G348C), Arg361 to Ser (R361S), Ala382 to Thr (A382T), Asn390 to Asp (N390D) and Asn390 to Ser (N390S) using a site-directed mutagenesis kit (Strategene). All constructs were verified by DNA sequencing.

Antibodies

A polyclonal TDP-43 antibody 10782-1-AP (anti-TDP-43) was purchased from ProteinTech Group Inc. A polyclonal antibody specific for phosphorylated TDP-43 (anti-pS409/410) and anti-405-414 antibody specific for C-terminal TDP-43 were prepared as described (15,19). Anti-ubiquitin monoclonal antibody (mAb), MAB1510, was purchased from Chemicon. Anti-GFP mAb, anti-RFP polyclonal antibody and agarose-conjugated anti-GFP were purchased from MBL (Nagoya, Japan). Monoclonal anti-alpha-tubulin and anti-p84 were obtained from Sigma and Abcam, respectively.

Cell culture and expression of plasmids

SH-SY5Y cells were cultured in DMEM/F12 medium (Sigma) supplemented with 10% (v/v) fetal calf serum, penicillin–streptomycin–glutamine (Gibco), and MEM Non-Essential Amino Acids Solution (Gibco). The cells were maintained at 37°C under a humidified atmosphere of 5% (v/v) CO_2. They were grown to 50% confluence in six-well culture dishes for transient expression and then transfected with expression plasmids using FuGENE6 (Roche) according to the manufacturer's instructions. Under our experimental conditions, the efficiency of transfection with pEGFP-C1 vector was 20–30%.

Confocal immunofluorescence microscopy

SH-SY5Y cells were grown on a coverslip (15 × 15 mm) and transfected with expression vector(s) (1 or 2 μg). After incubation for the indicated time, the transfected cells on the coverslips were fixed with 4% (w/v) paraformaldehyde in phosphate-buffered saline (PBS) for 30 min. The coverslips were then incubated in 50 mM NH_4Cl in PBS for 10 min and cell permeabilization was performed with 0.2% (v/v) Triton X-100 in PBS for 10 min. After blocking for 30 min in 5% (w/v) BSA in PBS, cells were incubated with anti-phosphorylated TDP-43 antibody, anti-pS409/410 (1:500 dilution) and anti-Ub (1:500) for 1 h at 37°C, followed by Alexa Fluor 488- or Alexa Fluor 568-labeled goat anti-rabbit or-mouse IgG (Invitrogen, 1:1000 dilution) for 1 h at 37°C. After washing, the cells were further incubated with TO-PRO-3 (Invitrogen, 1:3000 dilution in PBS) for 1 h at 37°C to stain nuclear DNA, and analyzed using an LSM5 Pascal confocal laser microscope (Carl Zeiss).

Intracellular aggregates of GFP-tagged TDP-43 fragments had much more intense fluorescence of GFP than diffusely expressed, GFP-tagged wild-type TDP-43 or GFP alone. Therefore, to quantify the cells with GFP-tagged TDP-43 aggregates, the laser power (at 488 nm for detection of GFP) was adjusted so that only the aggregates were detected (30).

Total intensity of GFP fluorescence detected at the threshold laser power and that of TO-PRO-3 fluorescence, the latter corresponding to the total number of cells, in a given field (~800 × 800 μm) were measured with LSM5 Pascal v 4.0 software (Carl Zeiss) and the ratios of cells with inclusions were calculated.

In the co-expression experiments with combinations of GFP-tagged TDP 162–414 or TDP 218–414 and DsRed-tagged wild-type TDP-43, the laser power (at 543 nm for detection of DsRed) was appropriately adjusted so that the signals did not overlap.

Sequential extraction of proteins and immunoblotting

SH-SY5Y cells were grown in six-well plates and transfected transiently with expression plasmids (1 μg). After incubation for the indicated time, cells were harvested and lysed in TS buffer [50 mM Tris–HCl buffer, pH 7.5, 0.15 M NaCl, 5 mM ethylenediaminetetraacetic acid (EDTA), 5 mM ethylene glycol bis (β-aminoethyl ether)-*N,N,N,N*-tetraacetic acid (EGTA) and protease inhibitor cocktail (Roche)]. The lysates were centrifuged at 290 000*g* for 20 min at 4°C, and the supernatant was recovered as the TS-soluble fraction. The TS-insoluble pellets were lysed in TS buffer containing 1% (v/v) Triton X-100 (TX) and centrifuged at 290 000*g* for 20 min at 4°C. The supernatant was collected as the TX-soluble fraction. The TX-insoluble pellets were further sonicated in TS buffer containing 1% (w/v) Sarkosyl (Sar) and incubated for 30 min at 37°C. The mixtures were centrifuged at 290 000*g* for 20 min at room temperature and the supernatant was recovered as the Sar-soluble fraction. The remaining pellets (insoluble in Sar) were lysed in SDS-sample buffer and heated for 5 min.

Subcellular fractionation was performed using NE-PER nuclear and cytoplasmic extraction reagents (Pierce) according to the manufacturer's instructions. SH-SY5Y cells were grown in six-well plates and transfected transiently with expression plasmids (1 μg). After incubation for 48 h, cells were harvested and fractionated into nuclear and cytoplasmic fraction using NE-PER.

Protein concentration was estimated using the BCA Protein Assay Kit (Pierce). Each sample (10 or 20 μg) was separated by 10 or 12% (v/v) SDS–PAGE using Tris–glycine buffer system, and proteins were transferred onto polyvinylidene difluoride membrane (Millipore). The blots were blocked with 3% (v/v) gelatin and incubated overnight with the indicated primary antibody in 10% (v/v) calf serum at an appropriate dilution (1:1000–5000) at room temperature. The membranes were washed and then incubated with a biotin-labeled secondary antibody (Vector) for 2 h or a horse radish peroxidase-labeled secondary antibody (BIO-RAD) for 1 h at room temperature. Signals were detected using the ABC staining kit (Vector) or ECL Plus Western Blotting Detection System (GE Healthcare).

CFTR exon 9 skipping assay

Cos-7 cells grown in six-well plates were transfected with 0.5 μg of the reporter plasmid pSPL3-CFTR9 (including a TG11T7 (16) or TG13T5 sequence) plus 1 μg of pEGFP plasmid encoding wild-type TDP-43 or its fragment, using FuGENE6. The cells were harvested 48 h post-transfection and total RNA was extracted with TRIzol (Invitrogen). The cDNA was synthesized from 1 μg of total RNA with the use of the Superscript II system (Invitrogen). Primary and secondary PCRs were carried out according to the instruction manual of the exon trapping system (Life Technologies).

Immunoprecipitation

SH-SY5Y cells grown in six-well plates were transfected with expression vectors (total 2 μg). After incubation for 3 days, cells were harvested and lysed in RIPA buffer [50 mM Tris–HCl buffer, pH 7.5, 0.15 M NaCl, 1% NP-40, 0.5% deoxycholic acid Na, 0.1% SDS, 5 mM EDTA, 5 mM EGTA, 1 mM PMSF and protease inhibitor cocktail (Roche)]. The lysates were centrifuged at 20 400*g* for 10 min at 4°C and the supernatant (total protein: ~100 μg) was recovered and subjected to IP with agarose conjugated anti-GFP [20 μl of 50% gel slurry (~5 μg of anti-GFP), MBL]. Bound proteins were washed with RIPA buffer and then eluted from the beads with SDS sample buffer. Each sample was separated by 10% SDS–PAGE and immunoblotted with anti-GFP mAb (MBL), anti-RFP polyclonal antibody (MBL) and anti-TDP-43 (ProteinTech).

Mass spectrometric analysis of C-terminal fragments of TDP-43

Sarkosyl-insoluble, 8 M urea soluble fractions prepared from the brain of patients with FTLD-U were subjected to reversed phase-HPLC on an Aquapore RP-300 column (4.6 × 30 mm, Brownlee columns) and fractionated samples were immunoblotted with anti-pS409/410. The positive fraction was lyophilized, treated with SDS-sample buffer and loaded on 15% SDS–PAGE. The pS409/410-positive ~23 kDa bands (Fig. 9A) were dissected and digested in-gel with trypsin. The digests were applied to the Paradigm MS4 HPLC system (Microm BioResources). A reversed phase capillary column (Develosil ODS-HG5, 0.075 × 150 mm, Nomura Chemical) was used at a flow rate of 300 nm/min with a 4–80% linear gradient of acetonitrile in 0.1% formic acid. Eluted peptides were directly detected with an ion trap mass spectrometer, LXQ (Thermo Electron). The obtained spectra were analyzed with BioWorks (Thermo Electron) and Mascot (Matrix Science).

Statistical analysis

The *P*-values for the description of the statistical significance of differences were calculated by means of the unpaired, two-tailed Student's *t*-test using Prism 4 software.

SUPPLEMENTARY MATERIAL

Supplementary Material is available at *HMG* online.

ACKNOWLEDGEMENTS

We thank Dr H. Mimuro (University of Tokyo) for helpful advice and discussions.

Conflict of Interest statement. None declared.

FUNDING

This work was supported by a Grant-in-Aid for Scientific Research on Priority Areas–Research on Pathomechanisms of Brain Disorders (to M.H., 20023038), and Grants-in-Aid for Scientific Research to M.H. (18300117) and F.K. (20300144) and to T.N. (19590297) and T.A. (19591024) from the Ministry of Education, Culture, Sports, Science and Technology of Japan.

REFERENCES

1. Snowden, J.S., Neary, D. and Mann, D.M. (2002) Frontotemporal dementia. *Br. J. Psychiatry.*, **180**, 140–143.
2. Arai, T., Hasegawa, M., Akiyama, H., Ikeda, K., Nonaka, T., Mori, H., Mann, D., Tsuchiya, K., Yoshida, M., Hashizume, Y. *et al.* (2006) TDP-43 is a component of ubiquitin-positive tau-negative inclusions in frontotemporal lobar degeneration and amyotrophic lateral sclerosis. *Biochem. Biophys. Res. Commun.*, **351**, 602–611.
3. Neumann, M., Sampathu, D.M., Kwong, L.K., Truax, A.C., Micsenyi, M.C., Chou, T.T., Bruce, J., Schuck, T., Grossman, M., Clark, C.M. *et al.* (2006) Ubiquitinated TDP-43 in frontotemporal lobar degeneration and amyotrophic lateral sclerosis. *Science*, **314**, 130–133.
4. Gitcho, M.A., Baloh, R.H., Chakraverty, S., Mayo, K., Norton, J.B., Levitch, D., Hatanpaa, K.J., White, C.L. III, Bigio, E.H., Caselli, R. *et al.* (2008) TDP-43 A315T mutation in familial motor neuron disease. *Ann. Neurol.*, **63**, 535–538.
5. Kabashi, E., Valdmanis, P.N., Dion, P., Spiegelman, D., McConkey, B.J., Vande Velde, C., Bouchard, J.P., Lacomblez, L., Pochigaeva, K., Salachas, F. *et al.* (2008) TARDBP mutations in individuals with sporadic and familial amyotrophic lateral sclerosis. *Nat. Genet.*, **40**, 572–574.
6. Sreedharan, J., Blair, I.P., Tripathi, V.B., Hu, X., Vance, C., Rogelj, B., Ackerley, S., Durnall, J.C., Williams, K.L., Buratti, E. *et al.* (2008) TDP-43 mutations in familial and sporadic amyotrophic lateral sclerosis. *Science*, **319**, 1668–1672.
7. Van Deerlin, V.M., Leverenz, J.B., Bekris, L.M., Bird, T.D., Yuan, W., Elman, L.B., Clay, D., Wood, E.M., Chen-Plotkin, A.S., Martinez-Lage, M. *et al.* (2008) TARDBP mutations in amyotrophic lateral sclerosis with TDP-43 neuropathology: a genetic and histopathological analysis. *Lancet. Neurol.*, **7**, 409–416.
8. Yokoseki, A., Shiga, A., Tan, C.F., Tagawa, A., Kaneko, H., Koyama, A., Eguchi, H., Tsujino, A., Ikeuchi, T., Kakita, A. *et al.* (2008) TDP-43 mutation in familial amyotrophic lateral sclerosis. *Ann. Neurol.*, **63**, 538–542.
9. Benajiba, L., Le Ber, I., Camuzat, A., Lacoste, M., Thomas-Anterion, C., Couratier, P., Legallic, S., Salachas, F., Hannequin, D., Decousus, M. *et al.* (2009) TARDBP mutations in motoneuron disease with frontotemporal lobar degeneration. *Ann. Neurol.*, **65**, 470–473.
10. Deng, H.X., Hentati, A., Tainer, J.A., Iqbal, Z., Cayabyab, A., Hung, W.Y., Getzoff, E.D., Hu, P., Herzfeldt, B., Roos, R.P. *et al.* (1993) Amyotrophic lateral sclerosis and structural defects in Cu,Zn superoxide dismutase. *Science*, **261**, 1047–1051.
11. Rosen, D.R., Siddique, T., Patterson, D., Figlewicz, D.A., Sapp, P., Hentati, A., Donaldson, D., Goto, J., O'Regan, J.P., Deng, H.X. *et al.* (1993) Mutations in Cu/Zn superoxide dismutase gene are associated with familial amyotrophic lateral sclerosis. *Nature*, **362**, 59–62.
12. Mackenzie, I.R., Bigio, E.H., Ince, P.G., Geser, F., Neumann, M., Cairns, N.J., Kwong, L.K., Forman, M.S., Ravits, J., Stewart, H. *et al.* (2007) Pathological TDP-43 distinguishes sporadic amyotrophic lateral sclerosis from amyotrophic lateral sclerosis with SOD1 mutations. *Ann. Neurol.*, **61**, 427–434.
13. Tan, C.F., Eguchi, H., Tagawa, A., Onodera, O., Iwasaki, T., Tsujino, A., Nishizawa, M., Kakita, A. and Takahashi, H. (2007) TDP-43 immunoreactivity in neuronal inclusions in familial amyotrophic lateral sclerosis with or without SOD1 gene mutation. *Acta. Neuropathol.*, **113**, 535–542.
14. Piao, Y.S., Wakabayashi, K., Kakita, A., Yamada, M., Hayashi, S., Morita, T., Ikuta, F., Oyanagi, K. and Takahashi, H. (2003) Neuropathology with clinical correlations of sporadic amyotrophic lateral sclerosis: 102 autopsy cases examined between 1962 and 2000. *Brain Pathol.*, **13**, 10–22.
15. Hasegawa, M., Arai, T., Nonaka, T., Kametani, F., Yoshida, M., Hashizume, Y., Beach, T.G., Buratti, E., Baralle, F., Morita, M. *et al.* (2008) Phosphorylated TDP-43 in frontotemporal lobar degeneration and amyotrophic lateral sclerosis. *Ann. Neurol.*, **64**, 60–70.
16. Nonaka, T., Arai, T., Buratti, E., Baralle, F.E., Akiyama, H. and Hasegawa, M. (2009) Phosphorylated and ubiquitinated TDP-43 pathological inclusions in ALS and FTLD-U are recapitulated in SH-SY5Y cells. *FEBS Lett.*, **583**, 394–400.
17. Winton, M.J., Igaz, L.M., Wong, M.M., Kwong, L.K., Trojanowski, J.Q. and Lee, V.M. (2008) Disturbance of nuclear and cytoplasmic TAR DNA-binding protein (TDP-43) induces disease-like redistribution, sequestration, and aggregate formation. *J. Biol. Chem.*, **283**, 13302–13309.
18. Ayala, Y.M., Zago, P., D'Ambrogio, A., Xu, Y.F., Petrucelli, L., Buratti, E. and Baralle, F.E. (2008) Structural determinants of the cellular localization and shuttling of TDP-43. *J. Cell Sci.*, **121**, 3778–3785.
19. Inukai, Y., Nonaka, T., Arai, T., Yoshida, M., Hashizume, Y., Beach, T.G., Buratti, E., Baralle, F.E., Akiyama, H., Hisanaga, S.I. *et al.* (2008) Abnormal phosphorylation of Ser409/410 of TDP-43 in FTLD-U and ALS. *FEBS Lett.*, **582**, 2899–2904.
20. Buratti, E., Dork, T., Zuccato, E., Pagani, F., Romano, M. and Baralle, F.E. (2001) Nuclear factor TDP-43 and SR proteins promote *in vitro* and *in vivo* CFTR exon 9 skipping. *EMBO J.*, **20**, 1774–1784.
21. Buratti, E. and Baralle, F.E. (2001) Characterization and functional implications of the RNA binding properties of nuclear factor TDP-43, a novel splicing regulator of CFTR exon 9. *J. Biol. Chem.*, **276**, 36337–36343.
22. Johnson, B.S., McCaffery, J.M., Lindquist, S. and Gitler, A.D. (2008) A yeast TDP-43 proteinopathy model: Exploring the molecular determinants of TDP-43 aggregation and cellular toxicity. *Proc. Natl Acad. Sci. USA*, **105**, 6439–6444.
23. Igaz, L.M., Kwong, L.K., Xu, Y., Truax, A.C., Uryu, K., Neumann, M., Clark, C.M., Elman, L.B., Miller, B.L., Grossman, M. *et al.* (2008) Enrichment of C-terminal fragments in TAR DNA-binding protein-43 cytoplasmic inclusions in brain but not in spinal cord of frontotemporal lobar degeneration and amyotrophic lateral sclerosis. *Am. J. Pathol.*, **173**, 182–194.
24. Buratti, E., Brindisi, A., Giombi, M., Tisminetzky, S., Ayala, Y.M. and Baralle, F.E. (2005) TDP-43 binds heterogeneous nuclear ribonucleoprotein A/B through its C-terminal tail: an important region for the inhibition of cystic fibrosis transmembrane conductance regulator exon 9 splicing. *J. Biol. Chem.*, **280**, 37572–37584.
25. Ayala, Y.M., Pantano, S., D'Ambrogio, A., Buratti, E., Brindisi, A., Marchetti, C., Romano, M. and Baralle, F.E. (2005) Human, Drosophila, and C.elegans TDP43: nucleic acid binding properties and splicing regulatory function. *J. Mol. Biol.*, **348**, 575–588.
26. Wang, H.Y., Wang, I.F., Bose, J. and Shen, C.K. (2004) Structural diversity and functional implications of the eukaryotic TDP gene family. *Genomics*, **83**, 130–139.
27. Igaz, L.M., Kwong, L.K., Chen-Plotkin, A., Winton, M.J., Unger, T.L., Xu, Y., Neumann, M., Trojanowski, J.Q. and Lee, V.M. (2009) Expression Of TDP-43 C-terminal fragments in vitro recapitulates pathological features of TDP-43 proteinopathies. *J. Biol. Chem.*, **284**, 8516–8524.
28. Zhang, Y.J., Xu, Y.F., Dickey, C.A., Buratti, E., Baralle, F., Bailey, R., Pickering-Brown, S., Dickson, D. and Petrucelli, L. (2007) Progranulin mediates caspase-dependent cleavage of TAR DNA binding protein-43. *J. Neurosci.*, **27**, 10530–10534.
29. Zhang, Y.J., Xu, Y.F., Cook, C., Gendron, T.F., Roettges, P., Link, C.D., Lin, W.L., Tong, J., Castanedes-Casey, M., Ash, P. *et al.* (2009) Aberrant cleavage of TDP-43 enhances aggregation and cellular toxicity. *Proc. Natl Acad. Sci. USA*, **106**, 7607–7612.
30. Nagai, Y., Tucker, T., Ren, H., Kenan, D.J., Henderson, B.S., Keene, J.D., Strittmatter, W.J. and Burke, J.R. (2000) Inhibition of polyglutamine protein aggregation and cell death by novel peptides identified by phage display screening. *J. Biol. Chem.*, **275**, 10437–10442.

Biochemical and Biophysical Research Communications 382 (2009) 405–409

Contents lists available at ScienceDirect

Biochemical and Biophysical Research Communications

journal homepage: www.elsevier.com/locate/ybbrc

Identification of casein kinase-1 phosphorylation sites on TDP-43

Fuyuki Kametani [a,*], Takashi Nonaka [a], Takehiro Suzuki [c], Tetsuaki Arai [b], Naoshi Dohmae [c], Haruhiko Akiyama [b], Masato Hasegawa [a]

[a] Department of Molecular Neurobiology, Tokyo Institute of Psychiatry, Tokyo Metropolitan Organization for Medical Research, Kamikitazawa 2-1-8, Setagaya-ku, Tokyo 156-8585, Japan
[b] Department of Psychogeriatrics, Tokyo Institute of Psychiatry, Tokyo Metropolitan Organization for Medical Research, Tokyo 156-8585, Japan
[c] Biomolecular Characterization Team, Advanced Development and Supporting Center, The Institute of Physical and Chemical Research (RIKEN), Hirosawa 2-1, Wako, Saitama 351-0198, Japan

ARTICLE INFO

Article history:
Received 5 March 2009
Available online 13 March 2009

Keywords:
TDP-43
Phosphorylation
Casein kinase-1
Frontotemporal lobar degeneration with ubiquitin-positive inclusions
Amyotrophic lateral sclerosis
Mass spectrometry

ABSTRACT

TAR DNA-binding protein of 43 kDa (TDP-43) is deposited as hyperphosphorylated cytoplasmic and intranuclear inclusions in brains of patients with frontotemporal lobar degeneration with ubiquitinated inclusions and amyotrophic lateral sclerosis. In this study, we identified 29 phosphorylation sites on recombinant TDP-43 that are phosphorylated by casein kinase-1 (CK1). Interestingly, 18 of them were located in the C-terminal glycine-rich region of TDP-43. Our results indicate that CK1-mediated phosphorylation may play a role in the pathogenesis of these diseases.

Introduction

TAR DNA-binding protein 43 (TDP-43), encoded by the *TARDBP* gene on chromosome 1, is a highly conserved, ubiquitously expressed nuclear protein. It regulates gene transcription, exon splicing, and exon inclusion [1–4], and is also a multifunctional RNA-binding protein [4]. Recently, TDP-43 was identified as a major disease-associated protein in frontotemporal lobar degeneration with ubiquitin-positive inclusions (FTLD-U) and in amyotrophic lateral sclerosis (ALS) [5,6]. We previously reported that deposited TDP-43 is abnormally phosphorylated, and several antibodies raised against synthetic phosphorylated TDP-43 peptides recognized the pathological structures in FTLD-U and ALS [7]. Immunoblot analysis with these antibodies showed that the Sarkosyl-insoluble fraction extracted from brains of patients with FTLD-U and ALS contains hyperphosphorylated TDP-43 with a molecular weight of 45 kDa, together with fragments of 18–28 kDa [7,8]. Similar characteristic band patterns were obtained in the case of cultured cells expressing mutant TDP-43 [9]. In an in vitro phosphorylation assay of recombinant TDP-43, the product(s) of casein kinase-1 (CK1) phosphorylation showed similar electrophoretic mobility to that of hyperphosphorylated TDP-43 present in the brains of patients with FTLD-U and ALS, suggesting that CK1 may be involved in the hyperphosphorylation of TDP-43 [7,8]. To date, however, there is little information about the sites of the putative CK1-mediated hyperphosphorylation on TDP-43. In this study, we identified multiple sites on recombinant TDP-43 that are phosphorylated by CK1; in particular, the C-terminal Gly-rich region of TDP-43 appears to have a favorable conformation for CK1-mediated phosphorylation.

Materials and methods

TDP-43 construct and in vitro phosphorylation of TDP-43. Human TDP-43 cDNA was subcloned into pRK172 expression vectors and transformed into *Escherichia coli* BL21 (DE3) [7]. Crude extracts from *E. coli* expressing human TDP-43 were applied to a heparin-Toyopearl column. The column was washed, and TDP-43 was eluted with 0.5 M NaCl solution. The eluate (partially purified TDP-43) was phosphorylated with CK1 (New England Biolabs, Beverly, MA) at 30 °C for 14 h.

SDS–polyacrylamide gel electrophoresis (PAGE) and in-gel digestion. Phosphorylated TDP-43 was separated by SDS–PAGE [7]. The band of phosphorylated TDP-43 was excised and soaked in 50 mM Tris–HCl, pH 8.0 containing 50% acetonitrile for 30 min. The gel was dried in a Speed-Vac (Savant) and incubated in 50 mM Tris–HCl, pH 8.0 containing 125–250 ng of modified trypsin

* Corresponding author. Fax: +81 3 3329 8035.
E-mail address: kametani@prit.go.jp (F. Kametani).

0006-291X/$ - see front matter © 2009 Elsevier Inc. All rights reserved.
doi:10.1016/j.bbrc.2009.03.038